Sequence Dependence of Energy Transfer in DNA Oligonucleotides

Da-Guang Xu and Thomas M. Nordlund
Department of Physics, University of Alabama at Birmingham, Birmingham, Alabama 35294-1170 USA

ABSTRACT The sequence, temperature, concentration, and solvent dependence of singlet energy transfer from normal DNA bases to the 2-aminopurine base in synthesized DNA oligomers were investigated by optical spectroscopy. Transfer was shown directly by a variable fluorescence excitation band at 260–280 nm. Adenine (A) is the most efficient energy donor by an order of magnitude. Stacks of A adjacent to 2AP act as an antenna for 2AP excitation. An interposed G, C, or T base between A and 2AP effectively blocks transfer from A to 2AP. Base stacking facilitates transfer, while base pairing reduces energy transfer slightly. The efficiency is differentially temperature dependent in single- and double-stranded oligomers and is highest below 0°C in samples measured. An efficiency transition occurs well below the melting transition of a double-stranded decamer. The transfer efficiency in the duplex decamer d(CTGA[2AP]TTCAG)$_2$ is moderately dependent on the sample and salt concentration and is solvent dependent. Transfer at physiological temperature over more than a few bases is improbable, except along consecutive A's, indicating that singlet energy transfer is not a major factor in the localization of UV damage in DNA. These results have features in common with recently observed electron transfer from 2AP to G in oligonucleotides.

INTRODUCTION

One of the important risk factors for a living organism is ultraviolet radiation (UVR), obvious and direct consequences of which include increased skin cancer and accelerated aging for humans (Randle, 1997; Fisher et al., 1997). Today, skin cancer risk in the human population is on the rise (Bergmanson and Sheldon, 1997; Urbach, 1997), though much of the research into basic photophysical mechanisms ceased 5–10 years ago. Because of its large absorbance at ~260 nm, DNA is a major cellular target of UVR. Photoproduct formation, cell killing, mutation induction, and tumorigenesis are closely related to the UVR absorbed by DNA. The energy absorbed by DNA is dissipated by various mechanisms, some of which involve single bases (e.g., monomeric damage and single-strand breaks), others of which involve interactions between adjacent bases (e.g., dimerizations), between nonadjacent bases (interstrand or intrastrand cross-links), or between DNA and associated proteins (DNA-protein cross-links).

UV irradiation generates many lesions in DNA molecules, mainly at 1,2-dipyrimidine sites (Varghese and Wang, 1967; Varghese, 1972; Patrick and Rahn, 1976). The two major photoproducts are the cyclobutane pyrimidine dimer and the dipyrimidine 6-4 photoproduct. In addition to the major dimeric photoproducts (T-T, T-C, C-T, and C-C), other dimeric photoproducts may also occur, such as thymine-adenine (T-A) or adenine-adenine (A-A) dimers. The relative induction of these photoproducts depends on wavelength, DNA sequence, and protein-DNA interaction.

Most excitation energy, however, leaves an excited base without causing a chemical reaction, through nonradiative deexcitation (the primary pathway), radiative decay, intersystem crossing, or transfer to an acceptor. Energy migration within a DNA molecule occurs when the excited state energy of DNA transfers from some specific position to another position along the DNA. Data show that singlet and triplet energy transfers occur at both low temperature (77 K) and room temperature (Gueron et al., 1974; Ballini et al., 1976; Vigny and Ballini, 1977; Georghiou et al., 1990; Ge and Georghiou, 1991a,b; Huang and Georghiou, 1992; Nordlund et al., 1993).

At room temperature, the nucleic acid bases can act as energy donors and energy acceptors. Processes have been reported that involve singlet-singlet energy transfer from the bases to added probes, either covalent (Burr et al., 1975), intercalated, or otherwise bound to DNA (Lerman, 1963; Weill and Calvin, 1963; Le Pecq and Paoletti, 1967; Sutherland and Sutherland, 1967). Nucleic acid bases can act as triplet acceptors from ketones (Lamola, 1969). Georghiou et al. studied the dependence of fluorescence anisotropy of polynucleotides on wavelength and concluded there is energy transfer between modified and unmodified DNA bases at room temperature (Georghiou et al., 1990; Ge and Georghiou, 1991a,b; Huang and Georghiou, 1992). By observing that the intensity of the normal-base excitation band in the 260–270-nm region varies with temperature, while the emission band is identical to that of 2-aminopurine (2AP), we have shown that there is singlet-singlet energy transfer from normal DNA bases to 2AP in the d[CTGA[2AP]TTCAG]$_2$ B-DNA duplex decamer and that transfer efficiency is temperature dependent (Nordlund et al., 1993). The specific base(s) acting as donor(s) could not

Received for publication 23 June 1999 and in final form 1 October 1999.
Address reprint requests to Dr. Thomas M. Nordlund, Department of Physics, University of Alabama at Birmingham, 310 Campbell Hall, 1300 University Blvd., Birmingham, AL 35294-1170. Tel.: 205-934-0340; Fax: 205-934-8042; E-mail: nordlund@uab.edu.
Dr. Xu's present address is Bockus Research Hospital, Philadelphia, PA.

0006-3495/00/02/1042/17 $2.00

be identified because of the similarity of the absorption spectrum of the normal bases.

Absorption of UV light results in photodamage to double- or single-helical DNA that is not random. The formation of the most common UV photoproduct, the thymine-thymine cyclobutane dimer, was observed to occur with a probability varying by a factor of up to 80 in the *lacI* gene (Brash and Haseltine, 1982). Brunk (1973) showed that thymine photodimers were more likely to form in long stretches of T rather than in short stretches. A study of the distribution of photodimers in UV-irradiated DNA of known sequence (Gordon and Haseltine, 1982) showed 1) that the probability of pyrimidine dimer formation depended upon the thymine (T) content of the site (i.e., TT is more likely to form a dimer than TC, and CT is more likely to form a dimer than CC), and 2) that the probability of dimer formation depends upon the two flanking bases, but that this information is not enough to explain differences in the observed damage. The authors proposed that other long-range sequence effects are involved. The overall probability of pyrimidine photodimer formation, as well as the distribution of the site-specific damage, can be the same for single-stranded as for double-stranded DNA, so double-helical geometry is not a prerequisite for damage. Rahn has shown that the dimer formation probability is highly temperature dependent for both duplex and single-stranded (denatured) DNA (Patrick and Rahn, 1976). The dimer formation probability in single-stranded (ss) DNA decreases linearly as temperature rises; the dimer formation probability in duplex DNA is constant below the melting temperature T_m = 80°C and decreases abruptly at T_m, approximately matching that in ssDNA. Gordon and Haseltine (1982) stated that the DNA sequence distribution of the dimer formation probability is the same for single-stranded as for double-stranded DNA, but the temperature was not specified. The pyrimidine-pyrimidine 6-4 photoproduct, which occurs with up to one-third the frequency of dimers (Mitchell, 1988), is more likely to form at TC and CC sites than at CT or TT sites in the *lacI* gene of *Escherichia coli* (Brash and Haseltine, 1982). The 6-4 product formation probability was claimed to be higher when the number of A-T base pairs located 5′ to the site increased and when an extended tract of pyrimidines located 5′ to the site was present (Wang, 1976, 1980; Hauswirth and Wang, 1977). Note, however, the distributions of cyclobutyl pyrimidine dimers and 6-4 lesions in the *lacI* gene of *E. coli* reveal that the sites of cyclobutane dimer formation do not correlate well with sites destined to mutate upon UV irradiation (Brash and Haseltine, 1982).

The upshot of these early studies is that UV damage does not simply occur at any base or pair of adjacent bases where light is absorbed, that T tends to be involved in damage, and that A tends to increase damage probabilities. There are several types of mechanisms that can explain the nonrandom distribution. One mechanism assumes that excited energy deposited at one site in the DNA helix can be transferred to other sites. The rate and direction of energy transfer depend upon the base sequence and the structure along the helix. To be of significance in explaining the large variation in damage rates at identical sites separated by many tens of bases, such transfer must occur over distances of more than a few adjacent bases. Energy transfer, either of singlet or of triplet excitation, has long been suggested as a possible cause of the preferential formation of photoproducts at specific sites in DNA (Setlow and Setlow, 1961; Gueron et al., 1967; Shafranovskaya et al., 1973; Frank-Kamenetskii and Lazurkin, 1974; Ballini et al., 1976; Suhai, 1984; Rubin and Yegupov, 1987; Georghiou et al., 1990). In this model, excitation energy would tend to accumulate at certain bases because of the variation in base-to-neighboring-base energy transfer rates and directions along the DNA helix. The weight of evidence has pointed toward triplet involvement in the formation of cyclobutane dimers but not in the 6-4 photoproducts (Hauswirth and Daniels, 1976; Patrick and Rahn, 1976; Umlas et al., 1985; Rubin and Yegupov, 1987).

Because the excited states of normal DNA bases predominantly have a very short lifetime, on the order of 10^{-11} s or less (Oraevsky et al., 1981; Ballini et al., 1982, 1988; Kobayashi et al., 1984; Georghiou et al., 1985; Rigler et al., 1985; Nordlund, 1988), the fluorescence of normal bases is very weak. This makes observation of energy transfer via fluorescence measurements difficult. 2-Aminopurine is a modified base that can be inserted into DNA and is an isomer of the normal base adenine (A), in which the exocyclic amino group is displaced from the 6- to the 2-position (Ward et al., 1969; Lycksell et al., 1987; McLaughlin et al., 1988). For the free mononucleoside in solution, this modification increases the fluorescence lifetime by three orders of magnitude to 10.0 ns and places the optical absorption and emission bands in a region clearly separated from that of the normal bases (Ward et al., 1969; Rigler and Claesens, 1986). Although the quantum yield of interior 2APs in DNA is much less than that of the free 2AP base (Ward et al., 1969; Gräslund et al., 1987; Lycksell et al., 1987; Millar and Sowers, 1990; Nordlund, 1988, 1990; Nordlund et al., 1989, 1990), the fluorescence of 2AP-containing DNA is high enough to easily measure under physiological conditions. 2AP still can form two hydrogen bonds with thymine in a double helix (Fig. 1), though one of the hydrogen bonds is moved from the major groove to the minor groove. Of critical importance is the observation that replacement of A by 2AP may not seriously disrupt the biological interactions of DNA: the 2AP-substituted duplex decamer, $d(CTGA[2AP]TTCAG)_2$, is recognized and cleaved by the *Eco*RI endonuclease, and the decamer indeed forms a B-like helix (McLaughlin et al., 1988; Nordlund et al., 1989). Reports on such biologically active, 2AP-containing DNA continually appear in the literature (Holz et al., 1998; Allan et al., 1999).

This study reports sequence-specific energy transfer between bases in model DNA molecules to determine 1)

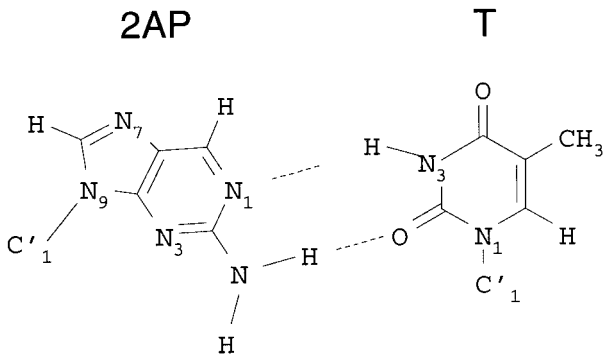

FIGURE 1 Base-pairing between 2AP and T. Picture generated by ISIS/Draw (Rev. 1.2W), MDL Information Systems.

whether such transfer can play a role in forming photoproducts at specific sites and 2) whether energy transfer can be used as a spectroscopic probe for local DNA structure. The data show that 1) transfer from normal bases to 2-aminopurine occurs but is restricted to distances of a few bases; 2) that adenine is an order of magnitude more efficient than other normal bases in transferring singlet energy to 2AP; 3) that a large transfer increase occurs as temperature is lowered below ~15°C, continuing well below −10°C; 4) that a (5′)G-2AP-C sequence has a unique fluorescence signature; 5) that the energy-transfer band is most sensitive to local stacking interactions; and 6) that the bases adjacent to 2AP can be identified through the properties of the energy-transfer spectral bands.

EXPERIMENTAL AND ANALYTICAL METHODS

Oligonucleotide design and preparation

The 2-aminopurine-containing duplex decamer d(CTGA[2AP]TTCAG)$_2$ is structurally well characterized, biologically active, and highly fluorescent and was therefore employed to initiate DNA energy transfer studies by measuring its fluorescence spectra. After knowing there indeed is energy transfer in the oligonucleotide, to find out which base is the major energy donor or whether all four normal bases have similar transfer efficiencies, the following single-stranded oligomers were synthesized: (AAAA[2AP]AAAAA), (GGGG[2AP]GGGGG), (CCCC[2AP]CCCCC), (TTTT[2AP]TTTTT), (CCA[2AP]CC), (CCG[2AP]CC), (CCT[2AP]CC), (CCC[2AP]CC). The hexamers allow study of transfer from the base 5′ to 2AP. Base C was chosen at the ends of the hexamers because of its low transfer efficiency (this project), because G can form a strong nonstacking electronic interaction with 2AP (this project) and because base T can base pair with A and 2AP, so that oligomers could form mismatched double strands. Knowing that base A is a major energy donor to 2AP, to determine whether the other three bases (G, C, and T) can block the energy transfer from base A to 2AP, we synthesized the following sample set: (CCAG[2AP]CC), (CCAC[2AP]CC), (CCAT[2AP]CC). To determine if energy transfer is bidirectionally symmetric (5′ ↔ 3′), we synthesized the following oligomer set: (CCA[2AP]CC), (CCA[2AP]ACC). To study how base pairing affects energy transfer efficiency, the following oligomer set was synthesized: (A[2AP]T) and (A[2AP]T/TTA); (AAAA[2AP]AAAAA) and (AAAA[2AP]AAAAA/TTTTTTTTTT). To determine if there is interstrand energy transfer from base A to 2AP between two strands, the following oligomers were used: (CCT[2AP]CC) and (CCT[2AP]CC/GGATGG). To investigate how sample concentration, salt, and solvent affect the energy transfer from normal bases (A, G, C, and T) to 2AP, the energy transfer efficiency of duplex decamer d(CTGA[2AP]TTCAG)$_2$ was studied 1) at different sample concentrations, 2) at different salt (KCl) concentrations, and 3) in a mixture of buffer and propylene glycol at different v/v ratios of propylene glycol.

All oligonucleotides containing the 2AP modified base were prepared with an Applied Biosystems 392 and 394 DNA/RNA synthesizer (Perkin Elmer, Applied Biosystems Division, Foster City, CA) on the 0.2-μmol or 1-μmol scale, using the standard cycle. The overall yield of synthesis was 99–99.5%. The concentration of the synthesized oligonucleotide solution was determined by measuring the absorbance at 260 nm.

Materials

To synthesize the 2AP-containing DNA oligomers, 2-aminopurine-CE phosphoramidate was purchased from Glen Research Corporation (Sterling, VA). Monomeric 2-aminopurine 2′-deoxynucleosides (2AP-dns) were generously provided by Dr. George W. Koszalka (Burroughs Welcome Co., Research Triangle Park, NC). Distilled deionized water was used to prepare solutions for fluorescence experiments.

A buffer consisting of 20 mM Tris-HCl, 0.1 M KCl, and 0.1 mM EDTA (pH 7.4) was used for all samples. Propylene glycol (U.S.P.-F.C.C. Baker analyzed grade) was purchased from J. T. Baker. The absorption coefficients of 2AP-dns at 260 nm and 305 nm were 1.85×10^3 and 7.21×10^3 M^{-1} cm^{-1}, respectively. The 2AP-dns solution spectrum was used as a reference in calculating energy transfer in the synthesized oligonucleotides. Absorption coefficients of oligomers were calculated based on the method and data from the *Handbook of Biochemistry and Molecular Biology* (Borer, 1975). When we calculated the absorption coefficients of synthesized DNA oligomers, the following absorption coefficients of dinucleotides were used: for dApd[2AP] and d[2AP]pdA, $\varepsilon_{260} = 8.13 \times 10^3$ M^{-1} cm^{-1}; for dGpd[2AP] and d[2AP]pdG, $\varepsilon_{260} = 6.33 \times 10^3$ M^{-1} cm^{-1}; for dCpd[2AP] and d[2AP]pdC, $\varepsilon_{260} = 4.43 \times 10^3$ M^{-1} cm^{-1}; and for dTpd[2AP] and d[2AP]pdT, $\varepsilon_{260} = 4.98 \times 10^3$ M^{-1} cm^{-1}, respectively.

Spectroscopy

Absorption spectra were measured on a Gilford Response II spectrophotometer. Temperature was controlled with a Gilford thermoelectric sample holder (Thermoset Accessory). When the temperature was at 5°C and below, water condensation on the sample cuvette was reduced by blowing nitrogen gas into the sample chamber. Data were stored digitally and transferred to a PC for analysis.

To study the base-to-base energy transfer in DNA at lower temperatures, a low-temperature device based on a Varian V-4557 variable-temperature accessory was designed and built. This low-temperature device was controlled with a V-4540 variable-temperature controller (Varian Associates, Palo Alto, CA). During the experiment, the temperature was controlled by current in the heating element and by the flow rate of N_2 gas, which is cooled by liquid N_2. When the sample temperature was in the range of −2.0°C to 50.0°C, the sample temperature was controlled by Lauda refrigerating circulators (RMS-6; Brinkmann Instruments, Westbury, NY). The sample temperature was measured simultaneously with a thermocouple (nickel-chromium versus copper-nickel) (Omega, Stamford, CT) and thermistor probe assembly (Omega). The thermocouple and thermistor probe were directly attached to the outside wall of the cuvette.

Fluorescence spectra were collected using a Perkin-Elmer LF-50 luminescence spectrometer. The sample temperature was controlled by the Lauda circulator or modified variable system described previously. To reduce the light scattering caused by the frozen sample, WG360 and KV370 filters were put in the front of the emission window for excitation spectra. Excitation and emission bandwidths were 2.5 and 5.0 nm, respectively. Data were stored, converted to Lotus 1-2-3 format, and transferred

to the PC for analysis. Excitation spectra were corrected for lamp fluctuations and monochromator wavelength dependence. Emission spectra were not corrected for wavelength-dependent efficiency of the detection system (emission monochromator and photomultiplier tube).

Data analysis

The average energy transfer efficiency from all donors to acceptor in a DNA oligonucleotide can be written (see Appendix A) as

$$\eta_t(\lambda_{ex}) = \frac{\sum_n^{N_X} \sum_X \varepsilon_X(\lambda_{ex}, n)\eta_X(\lambda_{ex}, n)}{\sum_n^{N_X} \sum_X \varepsilon_X(\lambda_{ex}, n)} = \frac{\sum_n^{N_X} \sum_X \varepsilon_X(\lambda_{ex}, n)\eta_X(\lambda_{ex}, n)}{\varepsilon(\lambda_{ex})} \quad (1)$$

Here, $\varepsilon_X(\lambda_{ex}, n)$ is the absorption coefficient of base X at position n in a single-stranded DNA oligonucleotide, and $\varepsilon(\lambda)$ is the total absorption coefficient of all energy donors (bases).

Calculation of energy transfer efficiency

Energy transfer from a donor molecule to an acceptor can be demonstrated by observing the emission at a wavelength characteristic of the acceptor and scanning the fluorescence excitation spectrum. Let $A_a(\lambda_a)$ be the absorbance of the acceptor (2AP) at its peak absorbance wavelength λ_a, let $A_a(\lambda_{ex})$ be the absorbance of the acceptor at any wavelength λ_{ex}, and let $A_d(\lambda_{ex})$ be the absorbance of the donor (normal DNA bases) at wavelength λ_{ex}. When excited at wavelength λ_{ex}, the transfer efficiency η_t from donor to acceptor is (see Appendix B)

$$\eta_t(\lambda_{ex}) = \frac{A_a(\lambda_{ex})}{A_d(\lambda_{ex})}\left[\frac{F(\lambda_{ex})}{F_a(\lambda_{ex})} - 1\right] \quad (2)$$

In oligonucleotides that contain the acceptor 2AP, the absorbance of the donors (normal bases) overlaps the absorbance of acceptor to a minor extent. The absorbance of the acceptor $A_a(\lambda_a)$ can be read directly from $A(\lambda_{ex})$, if normal bases do not absorb at λ_a (300–330 nm). The absorbance of the acceptor $A_a(\lambda_{ex})$ was obtained by measuring the absorption spectra of 2AP-dns, which must have the same concentration as 2AP in DNA oligonucleotides. The absorbance of donor $[A_d(\lambda_{ex})]$ at wavelength λ_{ex} was calculated by subtracting the absorbance of the acceptor (2AP) at λ_{ex} from the absorbance of DNA oligonucleotides at λ_{ex}.

The absorbances at 260 nm of the DNA oligonucleotides in our samples were higher than normally used in fluorescence spectroscopy. There are two reasons for this high absorbance: 1) accurate measurement of the low 307-nm absorbance necessitates a higher absorbance at 260 nm because measurements at the two wavelengths must be made at the same concentration and long-path-length cells cannot be used because of the sample cost, and 2) sample dilution would unacceptably depress the duplex melting temperature. Because of attenuation of the excitation beam through the sample, this relatively high absorbance at 260 nm will reduce the fluorescence intensity when excited at 260 nm. This reduction of the fluorescence intensity caused by attenuation of the excitation beam can be corrected by multiplying the measured fluorescence intensity at each excitation wavelength λ_{ex} by the factor

$$CF = \frac{2.303 * A(\lambda_{ex})}{1 - 10^{-A(\lambda_{ex})}} \quad (3)$$

The fluorescence spectra, corrected for high absorption, were normalized to 1 at wavelength λ_a, at which the spectra had peak intensity for direct excitation of 2AP. The absorbance of the energy donors (normal bases) was then calculated, as discussed above, and the energy transfer efficiency for single-stranded DNA oligonucleotides was calculated from Eq. 2. For double-stranded DNA oligonucleotides, the energy transfer efficiency $\eta(\lambda, T)$ at any temperature was calculated as in Appendix D. Because of the differential method for calculating spectral changes, a zero point of transfer was convenient and was chosen at the highest measured temperature, where transfer was the lowest (although perhaps not precisely zero).

Estimations of transfer efficiencies from individual nearest-neighbor and next-nearest-neighbor bases to the 2AP were made by assuming the efficiency of the nearest neighbor was not affected by the presence or absence of a next-nearest neighbor (Xu, 1996). For example, the efficiency of transfer from A in (CCAG[2AP]CC) can be obtained from the measured overall efficiency in this oligomer, assuming the G-to-2AP transfer is the same as that determined for G in (G[2AP]CC). This assumption of minor changes in interaction between G and 2AP induced by addition of bases CCA on the 5′ side could be incorrect in detail, but the individual base efficiencies could not otherwise be calculated.

RESULTS AND DISCUSSION

Evidence for energy transfer in synthesized DNA oligonucleotides

The UV absorption of 2AP containing DNA decamer $d(CTGA[2AP]TTCAG)_2$ is dominated by the absorbance of the normal bases in the 240–280-nm region because the absorbance of 2AP is very weak at 260 nm and the ratio of the number of the normal bases to 2AP is 9:1. The absorption of 2AP is small but clearly shows up as a shoulder near 307–315 nm (Xu et al., 1994). Comparison to an absorption spectrum of the unmodified $d(CTGAATTCAG)_2$ decamer allows accurate estimation of the absorbances of normal and 2AP bases at 260 and 307 nm. At 260 nm, 2AP contributes ~0.2% of the total absorbance. The fractional absorbance of normal bases at 307 nm is ~0.11, but this makes practically no contribution to fluorescence because of the low yield of normal base fluorescence and of transfer-excited 2AP fluorescence compared to directly excited 2AP fluorescence.

The normalized fluorescence excitation spectrum of the $d(CTGA[2AP]TTCAG)_2$ DNA decamer shows two changes with temperature (Nordlund et al., 1994; Fig. 2 *a*): 1) the position of the direct excitation peak of 2AP (near 307 nm) shifts to the red as the temperature decreases, and 2) a second excitation band in the 245–285-nm region appears at low temperature. The first of these changes has been attributed to progressively less exposure of the 2AP base to water as the helix goes below its melting temperature (Evans et al., 1992). The other change is the appearance of a new excitation band, which is most clearly evident below ~15°C and shows a peak at 250–280 nm (Nordlund et al., 1993). The observation of the new peak is in itself evidence that the fluorescence excited at 260 nm is not due to direct excitation of the 2AP base, because 2AP absorption is at a minimum at 260 nm and contributes only 0.2%. The magnitude of the new peak relative to the magnitude of direct excitation peak at 307 nm is greatest at about −12°C to −20°C (depending upon the decamer concentration), decreases to 75% to 80% of maximum, and stays constant as

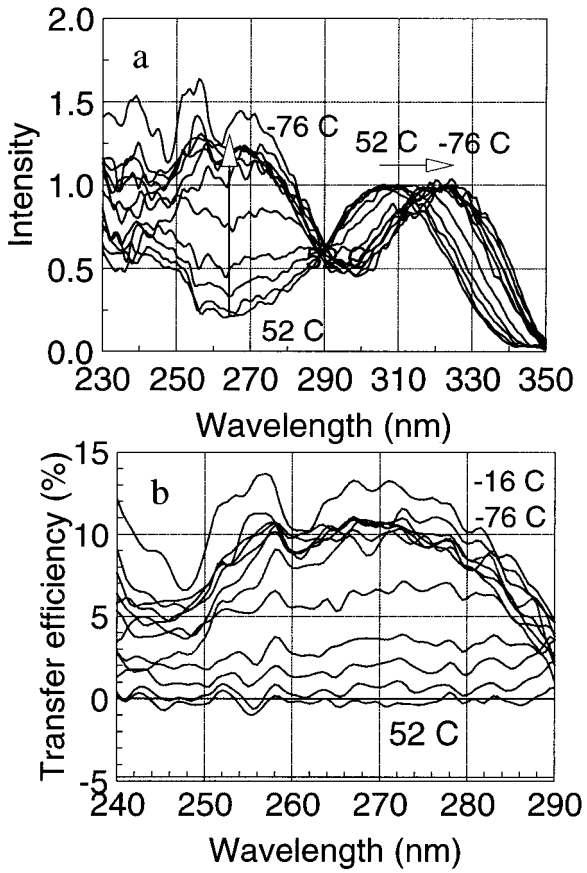

FIGURE 2 (*a*) Excitation spectra of the d(CTGA[2AP]TTCAG)$_2$ DNA decamer versus temperature, normalized to a direct-excitation peak amplitude of 1. The energy transfer band is evident in the 240–280-nm region. Duplex concentration 20 μM, 20 mM Tris-HCl, 0.1 M KCl, 0.1 mM EDTA, pH 7.4, emission wavelength 370 nm, excitation (emission) bandwidth 2.5 nm (5.0 nm). (*b*) Transfer efficiency spectra of the d(CTGA[2AP]TTCAG)$_2$. Efficiency spectra below 250 nm are distorted by the second excited-state band, above 280 nm, by the temperature-dependent shift of the 320–305-nm direct excitation band of 2AP. The higher noise in these data (compare Fig. 3) is caused by the lower fluorescence quantum yield in this duplex decamer (Nordlund et al., 1989; Nordlund, unpublished data).

the temperature decreases to about −75°C. (The increase in noise at low temperature is caused by scattering from the frozen sample.) At higher temperatures the peak decreases gradually, reaches its minimum at ~40°C, and increases again slightly from 40°C to 52°C. The excitation spectrum of the 2AP-dns base in buffer, on the other hand, has no peak in the 250–280-nm region. The excitation spectrum of 2AP-dns is temperature independent from 54°C to −26°C, except that the magnitude of the excitation spectrum in the 235–250-nm region increases by 17% as the temperature decreases. In the lowest temperature region, −26°C to −63°C, the magnitude of 235–250-nm excitation does not further increase, but the direct excitation peak of 2AP-dns shifts from 305 nm to 310 nm (Xu, 1996).

The transfer efficiency is related to the fluorescence intensity excited in the 250–280-nm region, but a zero-efficiency spectrum must be chosen. We assign zero transfer efficiency at the high temperature limit of the spectra, where the new peak is clearly near zero, and then subtract this limiting spectrum from that at each temperature to calculate the wavelength dependence of the efficiency. This high-temperature limit for the duplex decamer d(CTGA[2AP]TTCAG)$_2$ is 52°C in Fig. 2 *a*. The energy transfer efficiencies were calculated at each temperature and excitation wavelength and were plotted (Fig. 2 *b*). Fig. 2 *b* shows 1) the general increase in energy-transfer efficiency as the temperature decreases and 2) the approximate wavelength independence of the efficiency in the 255–280-nm region. Distortions in the outlying spectral regions are caused by overlap of other spectral bands.

The major energy donor is adenine

It is generally difficult to distinguish the contributions of each type of base by absorption and fluorescence spectra because their ultraviolet optical properties are quite similar (Voet et al., 1963; Gueron et al., 1974; Vigny and Ballini, 1977; Daniels and Hauswirth, 1971; Callis, 1979, 1983). For normal DNA bases, the absorption bands of individual monodeoxynucleotides at neutral pH are broad and peak at ~260 nm (A), ~266 nm (T), ~252 nm and ~275 nm (G), and ~270 nm (C). In the simplest case, the excitation spectrum of the energy transfer band should coincide with the absorption spectrum of the donor. The maximum in the excitation spectrum (Fig. 2) lies between 255 and 275 nm, but the intensity is within 10% of the maximum from 250 to 280 nm, so the particular base or bases acting as energy donor cannot be identified unambiguously only from spectral data.

To identify which base is acting as the energy donor, the single-stranded decamer d(AAAA[2AP]AAAAA) and analogous decamers with G, C, and T in place of A were examined. As shown in Fig. 3, the excitation peak with base A at 258 nm is 8–10 times higher than that with other bases. This indicates that energy transfer to 2AP is much more efficient from base A than from other bases (G, C, and T) in these oligomers. The transfer efficiency spectra (efficiency versus excitation wavelength) are calculated and shown in Fig. 4. The overall transfer efficiency (per base) from bases A to 2AP in single-stranded decamer d(AAAA[2AP]AAAAA) (η_A = 46% at 4°C) is about an order of magnitude higher than that from bases G, C, and T to 2AP in analogous decamers with G, C, and T in place of A (η_G = 5.1%, η_C = 5.3%, and η_T = 3.5%) (Table 1). The larger efficiency for A is further demonstrated by another set of 2AP-containing DNA hexamers: d(CCA[2AP]CC), d(CCG[2AP]CC), d(CCC[2AP]CC), and d(CCT[2AP]CC). Under the assumptions that energy transfer in these hexamers only occurs

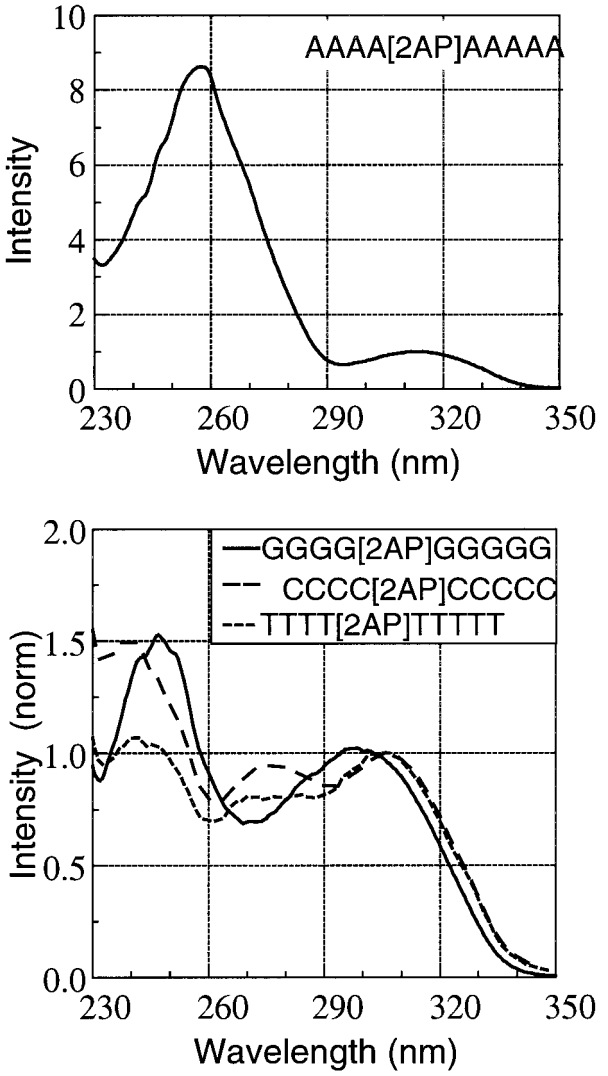

FIGURE 3 Excitation spectra of the single-stranded DNA decamers (XXXX[2AP]XXXXX, X = A, G, C, T, normalized to the direct excitation peak of 2AP. (*Top*) (AAAA[2AP]AAAAA), concentration 61 μM. (*Bottom*) (GGGG[2AP]GGGGG) (*solid line*), concentration 40 μM; (CCCC[2AP]CCCCC) (*dotted line*), concentration 67 μM; (TTTT[2AP]TTTTT) (*dash-dotted line*), concentration 64.5 μM. Emission wavelength 370 nm, excitation (emission) bandwidth 2.5 nm (5.0 nm); T = 3.5 ± 0.2°C.

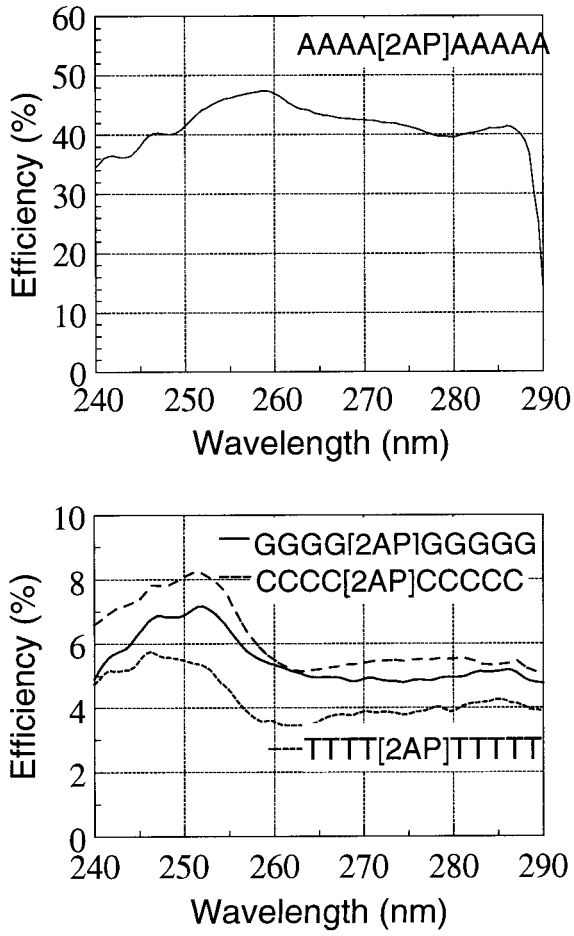

FIGURE 4 Transfer efficiency spectra of the single-stranded DNA decamers of Fig. 3.

from an excited base that is a nearest neighbor of 2AP and that C transfers equally well on either side of 2AP (see Appendix C), the transfer efficiency of a single left adjacent base to 2AP was calculated as follows: η(A) = 57%, η(G) = 19%, η(C) = 12%, and η(T) = 10% excited at 260 nm and 5.0°C (Table 2). These results imply that the energy transfer in the duplex decamer d[CTGA[2AP]TTCAG]$_2$ is mostly due to a highly efficient transfer from the adjacent base A to 2AP.

Transfer from an adjacent A to 2AP is equally efficient from the 5′ and 3′ sides of 2AP: 57 ± 5% at 5°C (Table 3).

Temperature dependence: base stacking facilitates transfer

To understand why transfer from A is much more efficient than from other bases, we examined the temperature-dependent absorption and excitation spectra of 2AP-containing single-stranded decamers with different bases. As a control, the fluorescence of 2AP-dns shows an excitation peak at

TABLE 1 Energy transfer efficiencies from A, G, C, and T to 2AP in ssDNA decamers

Samples	η_t (%)*	$\eta(-1)$ (%)†
(AAAA[2AP]AAAAA)	46 ± 5	
(GGGG[2AP]GGGGG)	5.1 ± 1.2	23 ± 3
(CCCC[2AP]CCCCC)	5.3 ± 0.9	24 ± 3
(TTTT[2AP]TTTTT)	3.5 ± 0.5	16 ± 1.5

T = 3.5°C, decamer concentrations 4–7 μM, λ_{ex} = 260 nm.
*Overall transfer efficiency from energy donor (normal base) to energy acceptor 2AP, calculated by Eq. 3.
†Transfer efficiency of the base positioned 5′ adjacent to 2AP, calculated as in Appendix C.

TABLE 2 Energy transfer efficiencies from A, G, C, and T to 2AP in ssDNA hexamers

Samples	η_t (%)	$\eta(-1)$ (%)
(CCA[2AP]CC)*	22 ± 2.5	57 ± 7
(CCG[2AP]CC)†	7.3 ± 0.9	19 ± 3
(CCC[2AP]CC)†	4.4 ± 0.7	12 ± 2.5
(CCT[2AP]CC)†	4.6 ± 0.8	10 ± 3

T = 5.0°C, λ_{ex} = 260 nm. See Table 1 footnotes.
*Single-stranded hexamer concentration 2.7 μM.
†Single-stranded hexamer concentration 50 μM.

305 nm, independent of temperature; the magnitude of its excitation peak increases by 14% above that at −1.7°C, reaching a maximum at 32°C and then falling by 12% when the temperature rises further to 54°C (data not shown). The mononucleoside spectrum thus has very little intrinsic temperature dependence.

d(AAAA[2AP]AAAAA)

The magnitude of the direct excitation peak of 2AP in this decamer increases rapidly, about fivefold, with temperature decreasing from 67°C to −1.7°C, and the direct excitation peak of 2AP shifts from 307 nm to 314 nm (Fig. 5). Base stacking is the major cause of hypochromism in DNA spectra, including this single-stranded sample, and of the 2AP excitation peak shift as temperature changes. At high temperature, the 2AP is more exposed to water, which is likely caused by high mobility of the base at high temperature (Nordlund et al., 1989; Xu et al., 1994).

d(GGGG[2AP]GGGGG)

The magnitude of the excitation peak of 2AP positioned between guanine bases increases by only 18% as the temperature decreases from 47°C to −2°C. Furthermore, the excitation peaks are all near 301 nm, an anomalously short wavelength (Fig. 6 *a*) (Evans et al., 1992). Because the magnitudes and positions of the 2AP excitation peaks in 2AP-dns are constant in this temperature regime, guanine must have a strong, probably nonstacking electronic interaction with 2AP. This strong nonstacking electronic interaction may be caused by a hydrogen bond between 2AP with base G, as the O atom at C6 of guanine can form an H-bond with a 2-amino hydrogen of 2AP (Evans, 1998). This interaction may be a facilitating factor in the electron transfer reported between 2AP and G (Kelley and Barton, 1999) in double-stranded oligomers.

TABLE 3 Energy transfer efficiencies of bases adjacent to 2AP in (CCA[2AP]CC) and (CCA[2AP]ACC) ssDNA oligomers

Sample	η_t (%)	$\eta(-1)$ (%)*	$\eta(+1)$ (%)†
(CCA[2AP]CC)‡	22 ± 2.5	57 ± 5	12 ± 2.5
(CCA[2AP]ACC)§	29 ± 3	57 ± 5	58 ± 6

T = 5.0°C, λ_{ex} = 260 nm. See Table 1 footnotes.
*Transfer efficiency of the base positioned 5′ adjacent to 2AP calculated as in Appendix C.
†Transfer efficiency of the base positioned 3′ adjacent to 2AP, calculated as in Appendix C.
‡Single-stranded hexamer concentration 2.7 μM.
§Single-stranded septamer concentration 50 μM.

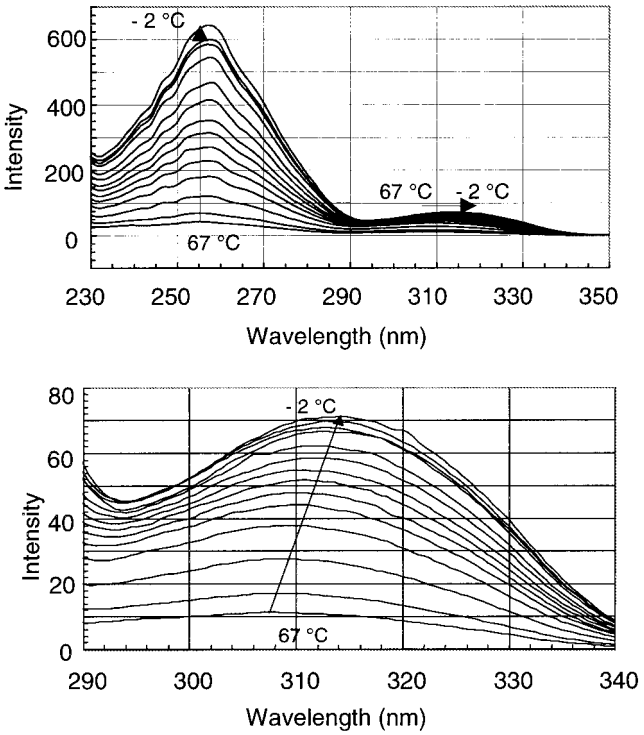

FIGURE 5 Temperature-dependent excitation spectra of the (AAAA[2AP]AAAAA) DNA decamer. Sample concentration 61 μM. (*Top*) Entire spectra. (*Bottom*) Enlargement of the 290–340-nm region. Emission wavelength 370 nm; excitation (emission) bandwidth 2.5 nm (5.0 nm). Note the large transfer band near 260 nm at low temperature, due to efficient transfer from A.

d(CCCC[2AP]CCCCC) and d(TTTT[2AP]TTTTT)

Although the magnitude of the excitation peak of 2AP in d(CCCC[2AP]CCCCC) and d(TTTT[2AP]TTTTT) DNA decamers increases by ~47% and ~36% as the temperature decreases from 47.3°C to −2.2°C, the magnitude of the low-temperature, direct excitation peak of 2AP in these decamers is much smaller than that in d(AAAA[2AP]AAAAA) and d(GGGG[2AP]GGGGG). Furthermore, the excitation peaks of 2AP in decamers d(CCCC[2AP]CCCCC) and d(TTTT[2AP]TTTTT) are all around 305–306 nm in the temperature range of −2.1°C to 47.0°C, approximately the same as those of 2AP-dns base in buffer (305 nm; Fig. 6, *b* and *c*). These results imply that bases C and T do not strongly stack with an adjacent base 2AP.

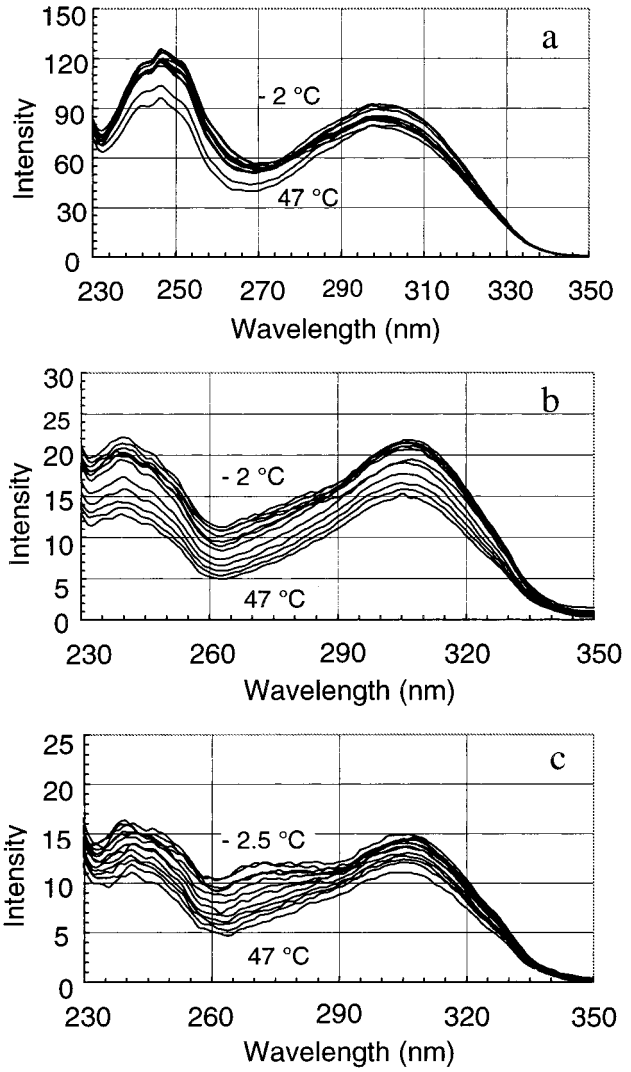

FIGURE 6 Temperature-dependent excitation spectra of ss decamers. (*a*) (GGGG[2AP]GGGGG) DNA decamer, concentration 40 μM. (*b*) (CCCC[2AP]CCCCC), 67 μM. (*c*) (TTTT[2AP]TTTTT), 65 μM. Emission wavelength 370 nm; excitation (emission) bandwidth 2.5 nm (5.0 nm).

Blockage of energy transfer from base A to 2AP

If adenine is the major energy donor to 2AP in DNA oligomers, do interposed bases G, C, and T, whose transfer efficiencies are ~10-fold less than that of A, block the transfer from A to 2AP? As shown in Table 4, the overall transfer efficiencies (for d(CCAG[2AP]CC), 6%; d(CCAC[2AP]CC), 5%; and d(CCAT[2AP)CC), 3%) are similar to those of d(CCX[2AP]CC) (Tables 2 and 3) and d(XXXX[2AP]XXXXX) (Table 1), where X = G, C, and T, and are much less than the 22% in d(CCA[2AP]CC). The calculated transfer efficiency of base A to 2AP in the above three samples is ~2%, ~6%, and ~0%, respectively, while the energy transfer efficiency of a second base A to the left side of 2AP in d(CCAA[2AP]CC) is ~16% (see also Appendix C). These results imply that the energy transfer from base A to 2AP is effectively blocked by a single interposed base G, C, or T.

TABLE 4 Energy transfer efficiencies in (CCAG[2AP]CC), (CCAC[2AP]CC), (CCAT[2AP]CC), and (CCAA[2AP]CC) DNA septamers

Sample	η_t (%)	$\eta(-1)$ (%)*	$\eta(-2)$ (%)†
(CCAG[2AP]CC)	6.3 ± 0.4	19 ± 3	2.0 ± 0.6
(CCAC[2AP]CC)	5.1 ± 0.5	12 ± 2.5	5.7 ± 1.1
(CCAT[2AP]CC)	3.0 ± 0.7	10 ± 3	−2.0 ± 2.5
(CCAA[2AP]CC)	20 ± 2.5	57 ± 7	16 ± 3

T = 5.0°C, oligomer concentrations 50 ± 1 μM, λ_{ex} = 260 nm. See Table 1 footnotes.
*Transfer efficiency of the base positioned 5′ adjacent to 2AP calculated as in Appendix C.
†Transfer efficiency of the base A positioned 5′ next adjacent to 2AP.

Because a stacking-type interaction seems crucial to energy transfer from A to 2AP and there is little stacking interaction between base 2AP and bases G, C, and T, a possible explanation for this transfer blockage is that the three-base stack, A-X-2AP, where X = G, C, or T, is loose compared to A-A-2AP. (Note that transfer even from the second-removed A in A-A-2AP is reasonably efficient at 16%.) Another explanation is that base A in the A-X-2AP sequence is somewhat farther away from 2AP or in a more unfavorable transfer orientation than the leftmost adenine in A-A-2AP. These speculations demand support from theoretical transfer mechanistic calculations, which we address later. The observation that stretches of A in one strand facilitate energy transfer to 2AP is similar to Kelley and Barton's data showing that electron transfer from photoexcited 2AP to G occurs with high efficiency with intervening A's, but not with other bases (Kelley and Barton, 1999).

Does presence of a complementary strand affect transfer?

To determine how base pairing affects the energy transfer, the efficiency in the single-stranded DNA decamer d(AAAA[2AP]AAAAA) was compared with that in the double-stranded decamer d(AAAA[2AP]AAAAA/TTTTTTTTTT). The formation of a double helix in DNA decamer d(AAAA[2AP]AAAAA/TTTTTTTTTT) was confirmed by its melting curve (data not shown). Table 5 shows that the overall energy transfer efficiency in the double-stranded decamer (20.5%) is somewhat less than that in the single-stranded oligomer (46%). Because there are about twice as many bases in the double-stranded DNA oligomer (10 T's and 9 A's) as in the single-stranded DNA oligomer (9 A's) and base T is not expected to contribute to energy transfer, the transfer efficiency from base A to 2AP must be nearly the same in both single- and double-stranded DNA oligomers. These results imply that formation of a double helix affects the energy transfer from A very little.

TABLE 5 Overall energy transfer efficiencies from normal bases to 2AP in ss and dsDNA oligomers

Sample	η_t (%)
A[2AP]T*	17.5 ± 1.5
A[2AP]T/TTA†	7.9 ± 0.8
AAAA[2AP]AAAAA‡	46 ± 5
AAAA[2AP]AAAAA/TTTTTTTTTT§	20.5 ± 2.5
CCT[2AP]CC¶	4.6 ± 0.4
CCT[2AP]CC/GGATGG‖	2.2 ± 0.3

$T = 5.0 \pm 0.5$°C, $\lambda_{ex} = 260$ nm. See Appendix D.
*Single-stranded trimer concentration 19 μM.
†Double-stranded trimer concentration 9.5 μM.
‡Single-stranded decamer concentration 6.1 μM.
§Double-stranded decamer concentration 2.9 μM.
¶Single-stranded hexamer concentration 50 μM.
‖Double-stranded hexamer concentration 39 μM.

To quantitate how forming a double helix affects the energy transfer in one strand of DNA, the theoretical value of the ratio, r, of average transfer efficiency from A in double-stranded DNA decamer d(AAAA[2AP]AAAAA/TTTTTTTTTT) to that from A in single-stranded DNA decamer d(AAAA[2AP]AAAAA) is compared with that of the experimental value. There are three cases (see Appendix D): $r > 0.60$, $r = 0.60$, and $r < 0.60$, corresponding to 1) $\eta_{s1}^{ds} > \eta_{s1}^{ss}$ (base pairing facilitates the energy transfer along one DNA strand), 2) $\eta_{s1}^{ds} = \eta_{s1}^{ss}$ (base pairing does not affect transfer), and 3) $\eta_{s1}^{ds} < \eta_{s1}^{ss}$ (base pairing reduces the efficiency of energy transfer). (Keep in mind that the transfer efficiency we speak of here will automatically decrease as the complementary strand of T's is added, independent of the effects of the second strand on the structure of the first strand, because T's absorb but do not transfer. What we are looking for is an effect on efficiency above or below this "automatic" decrease caused by the addition of more excitation absorbers.) The notation η_{s1}^{ds} (η_{s1}^{ss}) refers to the total transfer efficiency from all bases in strand 1 (A's in this case) in a double-stranded (single-stranded) oligomer. From experimental results, the ratio of transfer efficiency between these two is ($r = \eta^{ds}/\eta^{ss} = 0.45$, which corresponds to situation 3. This implies that base pairing of A's in d(AAAA[2AP]AAAAA) reduces the efficiency of energy transfer of those A's to 2AP by about one-quarter.

Does energy transfer from one strand to the other?

Armed with knowledge that forming a duplex does not facilitate the energy transfer, we can determine whether there is energy transfer between two complementary strands of DNA. If there is significant energy transfer between two complementary strands, the average transfer efficiency in d(CCT[2AP]CC/GGATGG) should be higher than ~2.3%, half of the 4.6% in the single-stranded d(CCT[2AP]CC) (Table 5). (Note that the adenine base, the most efficient donor, is as close as it can get to the 2AP in the opposite strand. This should maximize its transfer efficiency.) However, the efficiency found is 2.2% at 5°C. This suggests that there is little interstrand energy transfer in this oligomer. Following the procedure of the previous paragraph to quantitate the transfer, there are two cases, $r > 0.35$ and $r \leq 0.35$, corresponding to interstrand transfer occurring or not. The experimental results show that the ratio of transfer efficiency in the d(CCT[2AP]CC/GGATGG) duplex DNA hexamer to that in its single-stranded DNA hexamer d(CCT[2AP]CC) is $r = \eta^{ds}/\eta^{ss} = 0.48$. Based on these data, the calculated average transfer efficiency from the complementary strand d(GGATGG) is ~1.7% ± 0.3. The maximum transfer efficiency from base A in d(GGATGG) to 2AP in the complementary strand d(CCT[2AP]CC) is then found to be 7.7%, about one-eighth of the efficiency of base A when it is left-adjacent to the acceptor 2AP in a single-strand d(CCA[2AP]CC). These results indicate that interstrand energy transfer occurs, but with much less efficiency. (Note that observation of measurable transfer from A in the complementary strand to 2AP in d(GGATGG/CCT[2AP]CC) does not contradict the decrease in A → 2AP transfer in d(AAAA[2AP]AAAAA) caused by the presence of the complement d(TTTTTTTTTT).)

Estimation of transfer efficiencies in stacks of A

Table 6 shows the effect on the total transfer efficiency of inserting a progressively longer stretch of adenines to the 5′ side of 2AP. The slight total efficiency decrease as the number of A's goes from one to five indicates that the additional bases do, in fact, transfer energy to 2AP. If they did not transfer at all, the decrease would be more drastic, as the additional bases would absorb light but would not transfer. Appendix C describes our method for estimating the efficiency from each of the bases, the results of which are shown in Table 7. Although transfer from the nearest neighbor is by far the highest, transfer is measurable from the next four adenine bases. Table 7 suggests that transfer from the adenine four sites removed is anomalous. However, it

TABLE 6 Overall energy transfer efficiencies from normal bases to 2AP in DNA oligomers of different lengths

Sample	η_t (%)
(CCA[2AP]CC)*	21.5 ± 2.5
(CCAA[2AP]CC)†	20 ± 2
(CCAAA[2AP]CC)‡	17 ± 2
(CCAAAA[2AP]CC)§	16.5 ± 1.5
(CCAAAAA[2AP]CC)¶	16.5 ± 1.5

$T = 5.0$°C, $\lambda_{ex} = 260$ nm. See Table 1 footnotes.
*Single-stranded hexamer concentration 2.7 μM.
†Single-stranded septamer concentration 51 μM.
‡Single-stranded octamer concentration 7.0 μM.
§Single-stranded nonamer concentration 50 μM.
¶Single-stranded decamer concentration 51 μM.

TABLE 7 Energy transfer efficiencies from adenine bases at different positions relative to 2AP in ssDNA oligomers of different lengths

Sample	$\eta_A(-1)$ (%)*	$\eta_A(-2)$ (%)	$\eta_A(-3)$ (%)	$\eta_A(-4)$ (%)	$\eta_A(-5)$ (%)†
(CCA[2AP]CC)‡	57 ± 5				
(CCAA[2AP]CC)§	(57 ± 5)	16.5 ± 3.5			
(CCAAA[2AP]CC)¶	(57 ± 5)	(16.5 ± 3.5)	4.0 ± 0.8		
(CCAAAA[2AP]CC)‖	(57 ± 5)	(16.5 ± 3.5)	(4.0 ± 0.8)	15 ± 1	
(CCAAAAA[2AP]CC)**	(57 ± 5)	(16.5 ± 3.5)	(4.0 ± 0.8)	(15 ± 1)	15 ± 1
Förster calculation††	83	7.0	0.66	0.12	0.03

T = 5.0°C, λ_{ex} = 260 nm. See Table 1 footnotes. A number in parentheses is assumed to be equal to that in the oligomer above it in the table.
*The base A adjacent to the left side of 2AP.
†The fifth base A from the left side of 2AP.
‡Single-stranded hexamer concentration 2.7 μM.
§Single-stranded septamer concentration 51 μM.
¶Single-stranded octamer concentration 7.0 μM.
‖Single-stranded nonamer concentration 50 μM.
**Single-stranded decamer concentration 51 μM.
††From Xu (1996). Indicates the r^{-6} distance dependence of the Förster equation. Distances between bases are assumed to be 3.4 Å; angular factor random (κ^2 = 2/3).

should be noted that the results in this table rest on the assumption that an additional A does not affect the structure of the oligomer and the transfer of the other adenines. This assumption undoubtedly does not hold in detail, and Table 7 must be regarded as a "zeroth" approximation. Note that these calculations also do not address the mechanism, multistep or single-step, of transfer from these more remote bases.

Temperature dependence of energy transfer

The average transfer efficiency from base A to 2AP in the single-stranded decamer d(AAAAA[2AP]AAAA) decreases almost linearly from 48% to 16% as the temperature increases from −1.7°C to 72.4°C (Fig. 7). In the double-stranded decamer d(AAAA[2AP]AAAAA/TTTTTTTTTT), the melting temperature of which is ~12°C, the transfer efficiency decreases from 20% to 10% as the temperature rises from −2.4°C to 50.5°C (data not shown). Because the

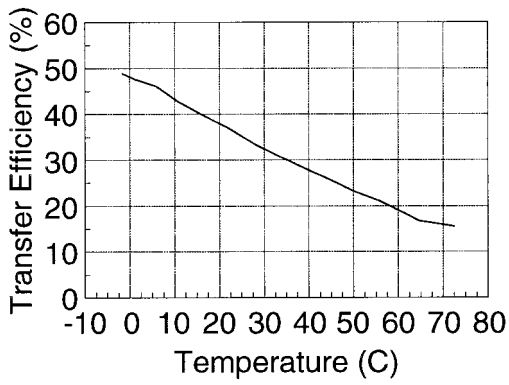

FIGURE 7 Transfer efficiency of ss (AAAA[2AP]AAAAA) as a function of temperature. λ_{ex} = 260 nm, single-stranded decamer concentration 6.1 μM.

overall transfer efficiency per donor base in single-stranded DNA decamer d(AAAA[2AP]AAAAA) (23% at T = 50.0°C, a temperature well above the 12°C melting temperature) is 2.3 times that in the corresponding "melted" double-stranded decamer (10.0% at T = 50.8°C), the melted duplex decamer must not be completely separated into two complementary single strands at 50.5°C. If the strands were completely unconnected, the transfer ratio would be 1/0.61 = 1.6 (Appendix D).

If, in a single-stranded DNA oligomer, base stacking is a primary factor governing energy transfer, disturbing the stacking interaction between bases in DNA may explain the temperature dependence of energy transfer. The base-stacking interaction decreases as temperature increases as the bases become more mobile (Gräslund et al., 1987; Nordlund et al., 1989). The linearity of the dependence likely reflects the fact that stacking associations within a single strand are not very cooperative.

The average transfer efficiency in double-stranded d(CTGA[2AP]TTCAG)$_2$ is also temperature dependent, but with a more complex behavior (Fig. 8). In the low temperature range from −76°C to −20°C, the efficiencies at different temperatures are almost constant (10 ± 3%), whereas in the middle range from −20°C to −10°C, there is an apparent transfer maximum of ~12% at −15°C, and finally, from −12°C to 52°C, the efficiency decreases dramatically from −12°C to 25°C and then more slowly from 25°C to 52°C. The reason for the maximum near −15°C is not clear. In this temperature range, the sample solution has just changed from liquid solution to solid ice. When freezing first occurs, solutes tend to aggregate; excluded from icy regions, the concentrated solutes locally depress the water freezing point. Transfer in the double-stranded decamer d(CAGT[2AP]TTCAG)$_2$ in a mixture of 50% buffer and 50% propylene glycol, which forms a glass at low temperature, does not show any comparable bump (Fig. 8), sug-

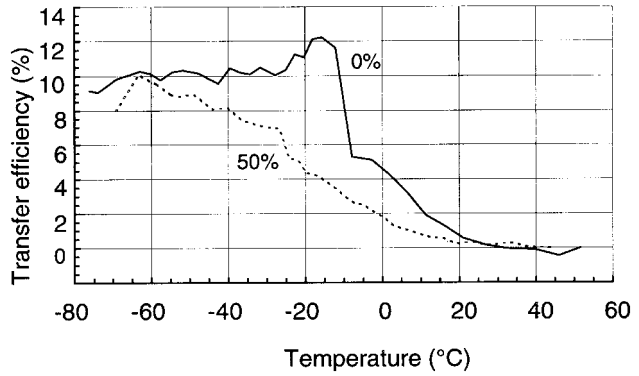

FIGURE 8 Transfer efficiency of d(CTGA[2AP]TTCAG)$_2$ duplex DNA decamer as a function of temperature in aqueous propylene glygol solution. The solid line is for a sample in aqueous buffer; the dotted line is for a sample in a mixture of 50% aqueous buffer and 50% propylene glycol. Duplex concentrations 20 μM, λ_{ex} = 265 nm.

gesting an anomaly caused by water freezing. In the very low temperature range (−76°C to −20°C), the constant transfer efficiency is consistent with unchanging base stacking resulting from freezing of the bases in place.

As shown in Figs. 8 and 9, and as we have noted before (Xu et al., 1994; the present data greatly extend the temperature range of that previous work), the average transfer efficiency versus T curve of normal bases to 2AP in the duplex decamer d(CAGT[2AP]TTCAG)$_2$ is S-shaped. The fact that the temperature corresponding to its midpoint of the curve (~0°C) is well below the melting temperature of the duplex decamer (~28°C) shows that the transition is not part of the normal cooperative double-helix formation, but rather part of a premelting transition. This premelting transition must not change the time-averaged structure of the oligonucleotides, which determines the absorption spectrum. We have proposed that the 2AP and other bases pass through a "mobility transition" 20°C or more below the melting temperature, which does not affect the bases' absorption (Xu et al., 1994). However, increased base mobility with rising temperature disturbs stable stacking and decreases the energy transfer between bases in DNA oligomer. As energy transfer involves base-base interaction in the excited state, as opposed to the ground-state interaction responsible for hypochromicity, the lower-temperature premelting temperature may reflect less stable stacking of an *excited* base.

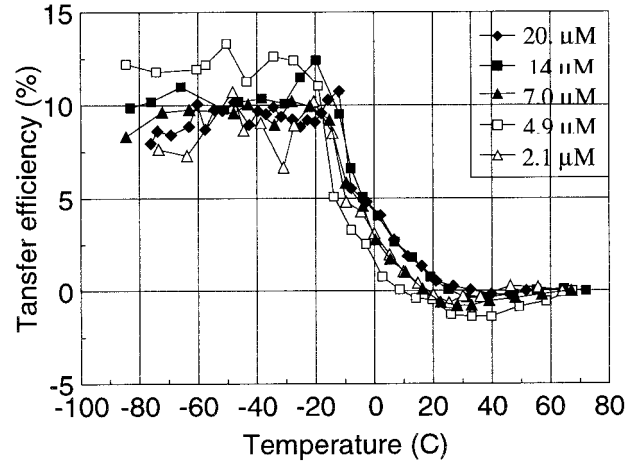

FIGURE 9 Duplex concentration dependence of transfer efficiency of d(CTGA[2AP]TTCAG)$_2$ as a function of temperature; λ_{ex} = 260 nm. Sample concentrations (duplex) are (in μM) 20, 14, 7.0, 4.9, and 2.1. Buffer: Tris-HCl 20 mM, KCl 0.1 M, EDTA 0.1 mM, pH 7.4.

Increased donor lifetime with decreasing temperature can, in principle, explain increased transfer efficiency. However, the present data, with a wide variety of temperature-dependent behaviors for the variety of structurally different oligomers in various solvents at various concentrations, cannot be explained by the same temperature dependence of donor lifetime. In addition, temperature-dependent measurements of normal base fluorescence show that normal base fluorescence continues to increase down to 77 K (Bloomfield et al., 1974), rather than stabilizing at −20°C, as our transfer efficiencies do.

Concentration dependence of energy transfer in duplex DNA

Transfer efficiencies show no regular dependence on duplex concentration at low temperature (−80°C to −20°C) or at high temperature (>30°C). At intermediate temperatures (−5°C to 25°C), higher concentration samples have somewhat higher transfer efficiencies (Fig. 9). The trend of the transfer efficiency data (higher transfer efficiency for higher concentrations) suggests that, at 2.0-μM duplex concentration with 0.1 M KCl, the double-stranded helix is indeed formed but is less stable and more mobile. (The present data do not rule out single-strand hairpin structures.) Although the transfer efficiency versus temperature curve shows that the transfer efficiency between bases is DNA concentration dependent, the magnitude of the transfer efficiency for duplex decamer d(CTGA[2AP]TTCAG)$_2$ changes only from 2.5% to 3.8% from concentration 4.9 μM to 20 μM (0.1 M KCl and T = 2°C). This is understandable because intramolecular energy transfer should not be affected by nearby duplex molecules, as long as the concentration is not high enough to change the aggregation state of the DNA.

Salt dependence of energy transfer

As shown in Fig. 10, the high-salt concentration sample has only moderately higher transfer efficiency in the transition-temperature region. Fig. 11 shows the normalized excitation spectra of the duplex decamer d(CTGA[2AP]TTCAG)$_2$ at different salt concentrations. The direct fluorescence excitation peak of 2AP shifts slightly to the red with increasing

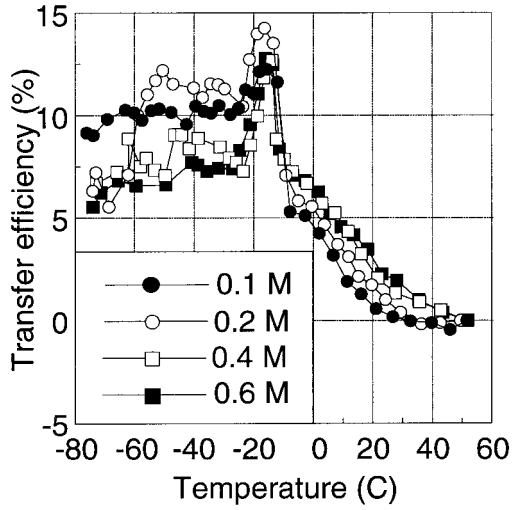

FIGURE 10 Temperature and salt dependence of transfer efficiency of d(CTGA[2AP]TTCAG)$_2$ DNA decamer excited at a wavelength of 265 nm. ●, Sample concentration 20.1 μM, KCl concentration 0.1 M; ○, sample concentration 19.7 μM, KCl 0.2 M; □, sample concentration 19.3 μM, KCl 0.4 M; ■, sample concentration 19.3 μM, KCl 0.6 M. Buffer: Tris-HCl 20 mM, KCl 0.1 M, EDTA 0.1 mM, pH 7.4. See text.

salt concentration. This agrees with results reported by Evans et al. (1992) and is attributed to the 2AP base being exposed less to water as the double helix is stabilized by increasing salt concentration. The amplitude of the 260–285-nm excitation band at 3°C increases by ~20% from 0.1 M to 0.6 M KCl. Although the transfer efficiency versus T curve shows that the energy transfer from normal bases to 2AP in duplex decamer d(CTGA[2AP]TTCAG)$_2$ is salt concentration dependent, the magnitude of the transfer efficiency changes only from 3.6% to 5.3% from salt concentration 0.1 M to 0.6 M (for 20 μM DNA concentration, T = 5°C). Apparently the salt concentration above 0.1 M does not affect the energy transfer very much.

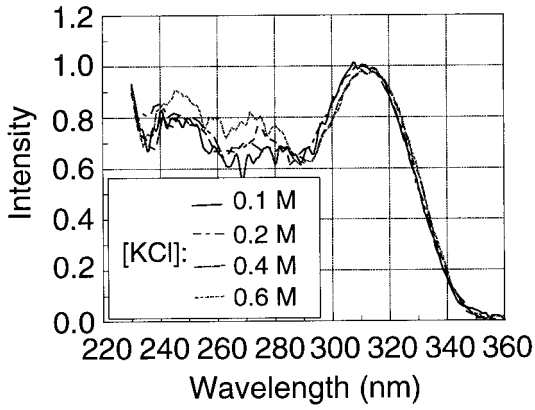

FIGURE 11 Salt dependence of excitation spectra of d(CTGA[2AP]TTCAG)$_2$ DNA decamer, normalized to a peak amplitude of 1. The solid line is for a sample concentration of 20.1 μM and a salt (KCl) concentration of 0.1 M; the dashed line is for a sample concentration of 19.7 μM and a salt (KCl) concentration of 0.2 M; the dotted line is for a sample concentration of 19.3 μM and a salt (KCl) concentration of 0.4 M; the dash-dotted line is for a sample concentration of 19.3 μM and a salt (KCl) concentration of 0.6 M. T = 3°C. Buffer: Tris-HCl 20 mM, KCl 0.1 M, EDTA 0.1 mM, pH 7.4. Emission wavelength 370 nm, excitation bandwidth 2.5 nm, emission bandwidth 5.0 nm. See text.

Solvent dependence of energy transfer

The fluorescence spectra of many fluorophores are sensitive to the polarity of their surrounding environment. Although the emission peak of 2AP in duplex decamer d(CTGA[2AP]TTCAG)$_2$ is the same (~369 nm) for different solvents, the magnitude of the emission peak increases as the fraction of propylene glycol increases (Fig. 12 *a*). This implies that the fluorescence quantum yield of 2AP increases as the fraction of propylene glycol increases. The excitation spectra of the d(CTGA[2AP]TTCAG)$_2$ decamer in pure buffer and in a mixture of 10% propylene glycol

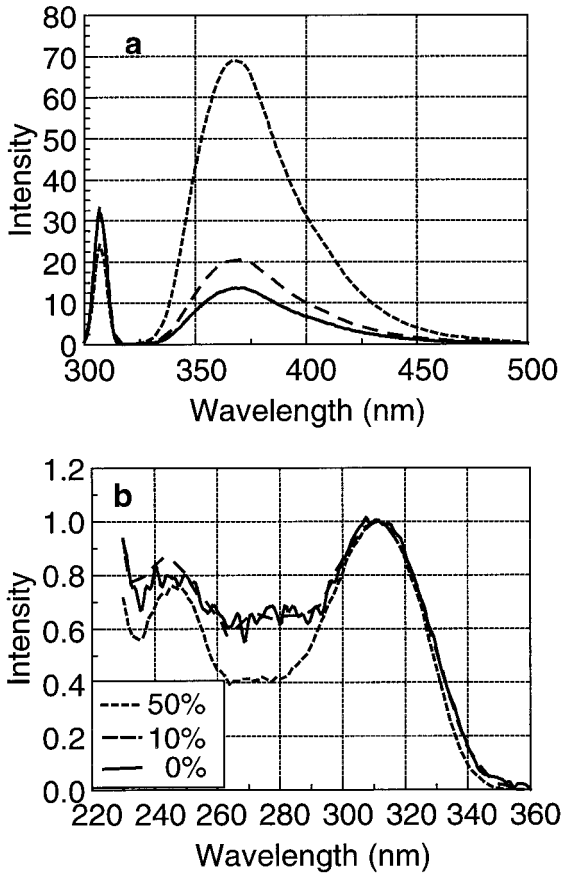

FIGURE 12 Fluorescence spectra of d(CTGA[2AP]TTCAG)$_2$ DNA decamer in a mixture of buffer and propylene glycol. (*a*) Emission spectra. (*b*) Excitation spectra, normalized to a peak amplitude of 1. The solid line is for pure buffer, sample concentration (duplex) 20.1 μM; the dashed line is for a mixture of 90% buffer and 10% propylene glycol, sample concentration (duplex) 20.6 μM; and the dotted line is for a mixture of 50% buffer and 50% propylene glycol, sample concentration 20.0 μM. The temperature is 3.0°C.

with 90% buffer are almost identical, whereas that in a mixture with 50% propylene glycol is different. The wavelengths of the direct excitation peak of 2AP in the decamer in three glycol concentrations (0%, 10%, and 50%) are the same (310 nm). Combined with the result that the emission peaks of 2AP in the three solvents are also the same (369 nm), we conclude that propylene glycol does not change the environment of 2AP enough to alter its electronic energy levels. However, the 260–285-nm excitation (energy transfer) bands in the 50% glycol mixture are much lower (~40%) than those in pure buffer or in the 10% mixture. Apparently 50% propylene glycol, but not 10%, disturbs the base stacking between base A and 2AP enough to reduce fluorescence quenching of 2AP. Higher solvent polarity introduces stronger hydrophobic forces between biomolecules and solvent. The dielectric constant of propylene glycol (37.7) is about half that of water (78.5). Thus, introducing more propylene glycol will reduce hydrophobic forces. The hydrophobic force is the major factor stabilizing the stacking interaction between bases in aqueous solution. Because the stacking interaction facilitating the energy transfer between bases in DNA oligomers decreases as propylene glycol concentration increases, the energy transfer from normal bases to 2AP in DNA oligomer should also decrease, as we observe.

SUMMARY AND CONCLUSION

Optical excitation of normal bases in dsDNA, e.g., $d(CTGA[2AP]TTCAG)_2$, can result in fluorescence emission from the incorporated 2-aminopurine base. The fluorescence emission spectrum is identical to that of directly excited 2-aminopurine, while an excitation peak in the 260–270-nm region, where normal bases absorb but 2AP does not, indicates that energy transfer takes place. The data show that transfer occurs most efficiently below ~10°C, where the bases stack best. Base stacking is expected to decrease as temperature increases and the double helix changes to single strands, although single strands can have stacked bases (Sänger, 1984). Adenine is a more efficient energy donor than G, C, and T by about an order of magnitude. Simplistic statistical models show that transfer from an adenine adjacent to 2AP is 57% at 5°C and close to 100% efficient in the low temperature limit. Average efficiencies for similar G-, C-, and T-containing oligomers are 3–5%, with efficiencies from bases adjacent to 2AP 16–24% at 5°C. Spectral evidence of the ability of adjoining adenines to interact when excited can be found in early studies of fluorescence from nucleic acids (Vigny and Ballini, 1977) and in recent measurements of electron transfer through adenine stacks to 2AP (Kelley and Barton, 1999).

Excitation energy transfers equally well from A situated to the 5′ or 3′ side of 2AP in ssDNA oligomers. Data show that a single interposed base G, C, or T effectively blocks the energy transfer from base A to base 2AP. The average transfer efficiency per donor of base A in a d(AA. . .A[2AP]A. . .A) ss oligomer decreases as the number of A bases increases.

The average transfer efficiency from normal bases to 2AP in a double-stranded DNA oligomer, d(AAAA[2AP]AAAAA/TTTTTTTTTT), is somewhat less than half that in single-stranded oligomer, d(AAAA[2AP]AAAAA). Base pairing reduces, by about one-quarter, energy transfer along the strand of the oligomer that contains the 2AP base. In ds d(CCT[2AP]CC/GGATGG) analysis shows that bases in the complementary strand, especially the most important donor base A, transfer measurably to 2AP.

The energy transfer efficiency is temperature dependent in both single- and double-stranded DNA oligomers. In a single-stranded DNA oligomer d(AAAA[2AP]AAAAA), the transfer efficiency decreases nearly linearly from 49% to 16% as the temperature rises from −2°C to 72°C, whereas in the double-stranded DNA oligomer d(AAAA[2AP]AAAAA/TTTTTTTTTT), with a melting temperature of ~12°C, the transfer efficiency decreases from 20% to 10% as the temperature rises from −2°C to 50°C. Transfer efficiencies in the ss and the ds oligomer at 50°C demonstrate that a "melted" double strand is not equivalent to completely separated single strands. The temperature dependence of energy transfer between bases in DNA must be related to base stacking, which is temperature dependent. However, the S-shaped transfer efficiency versus T curve of the duplex decamer $d(CTGA[2AP]TTCAG)_2$ indicates that there is a premelting transition in the duplex decamer, because the transition takes place well below the melting transition, extending to temperatures below 0°C. Temperature dependence of the donor (normal-base) lifetime, in the picosecond to subpicosecond regime at room temperature (Nordlund, 1990, 1991; Ballini et al., 1982, 1988; Georghiou et al., 1985; Callis, 1979), cannot explain the observed transfer versus temperature behavior. Temperature-dependent base mobility, with a low-mobility conformation favoring the excited-state, energy-transfer interaction, seems to be the primary player in this premelting transition.

Data for energy transfer in the $d(CTGA[2AP]TTCAG)_2$ duplex decamer show that in the transition temperature region, the transfer efficiency is moderately dependent upon the sample concentration (1–20 μM) and salt concentration. The effects of salt or DNA concentration amount to about ±1% out of a total transfer efficiency of 2–5%. Energy transfer efficiency between bases is likewise solvent dependent. The mechanism by which 50% propylene glycol reduces energy transfer between the bases is likely the reduction of the stacking interaction between bases, which are largely stabilized by hydrophobic forces.

The present results are direct experimental evidence of energy transfer in DNA oligomers and confirm that UV singlet-singlet energy transfer is a possible mechanism for the movement of energy in DNA, especially in stacks of adenine. The energy transfer in single-stranded DNA oligomers decreases almost linearly with increasing tempera-

ture above 0°C, agreeing with thymine dimer formation probability in heat-denatured DNA, but the temperature dependence of energy transfer in the duplex decamer d(CTGA[2AP]TTCAG)$_2$ does not agree with the temperature dependence of thymine dimer formation in native DNA (Patrick and Rahn, 1976). Because of the low absolute transfer efficiency at physiological temperature, because the energy transfer between bases in DNA decreases with the distance from the acceptor, and because transfer along stacks of A to 2AP is far more efficient than from C, T, or G, it is doubtful that excitation energy could transfer over more than a few bases. Therefore, it seems unlikely that the energy transfer reported here could play a significant role in the localization of any major types of UV damage in native DNA molecules.

Energy transfer to 2AP is facilitated by stacks of consecutive adenine bases. Kelley and Barton (1999) similarly observed that photoexcited electron transfer from 2AP to G is facilitated by stacks of A. An interesting possibility is that energy transfer from G to 2AP is followed by electron transfer back to G. 2AP fluorescence would be quenched, but this would not greatly affect our energy transfer calculation, which always normalizes for fluorescence yield. (We discuss in Nordlund et al. (1994) the effect of transfer to only a minority, short-lived 2AP state. Calculated transfer efficiency increased by at most a factor of 2 or so in that example.) Recent theoretical work (Kakitani et al., 1999) suggests that if energy transfer between A's occurs via intermediate coupling, a similarity in excitation transfer and electron transfer is expected. Whether or not intermediate coupling is appropriate for energy transfer from A to A and from A to 2AP, it seems clear that stacks of adenine can act as efficient conduits for energy and charge motion in DNA, at least over distances of 1–10 bases.

APPENDIX A: DEFINING THE ENERGY TRANSFER EFFICIENCY

If light of intensity I_0 (number of photons per second) and wavelength λ_{ex} illuminates a sample of absorbance $A(\lambda_{ex})$, the number of photons absorbed (per second) is

$$\Delta I = I_0(1 - 10^{-A(\lambda_{ex})}). \tag{A1}$$

If $\varepsilon_X(\lambda_{ex}, n)$ is the absorption coefficient and $A_X(\lambda_{ex}, n) = \varepsilon_X(\lambda_{ex}, n)c\ell$ is the absorbance of base X at position n in a single-stranded DNA molecule, the number of photons absorbed per second by this particular base X is

$$\Delta I_X(\lambda_{ex}, n) = \frac{A_X(\lambda_{ex}, n)}{A(\lambda_{ex})} I_0(1 - 10^{-A(\lambda_{ex})}), \tag{A2}$$

where c is the concentration of the oligomer and ℓ is the light path length. The total absorbance of all bases in the oligomer is

$$A(\lambda_{ex}) = \sum_X \sum_n^{N_X} A_X(\lambda_{ex}, n) = c\ell\varepsilon(\lambda_{ex}), \tag{A3}$$

where N_X is the number of bases X in a single-stranded DNA oligonucleotide and $\varepsilon(\lambda_{ex})$ is the total absorption coefficient. The summation symbol $\Sigma_n^{N_X}$ indicates that for each base of type X, the absorbance at each of the N_X base sites n occupied by X should be added.

The relative probability that a photon is absorbed by a particular donor X is

$$p_X(n) = \frac{A_X(\lambda_{ex}, n)}{A(\lambda_{ex})}. \tag{A4}$$

The transfer efficiency η_t can be defined as

$$\eta_t \equiv \frac{\text{Number of excited donors that result in excitation of acceptor}}{\text{Total number of excited donors}}.$$

If we define the efficiency of transfer from an energy donor X at position n in a single-stranded DNA to an acceptor as $\eta_X(\lambda_{ex}, n)$, then the average transfer efficiency, per donor, from donors (bases) to the acceptor in a single-stranded DNA is

$$\eta_t(\lambda_{ex}) = \frac{\Sigma_X \Sigma_n^{N_X} \varepsilon_X(\lambda_{ex}, n)\eta_X(\lambda_{ex}, n)}{\varepsilon(\lambda_{ex})}. \tag{A5}$$

$\eta_t(\lambda_{ex})$ is, in principle, dependent upon the excitation wavelength.

APPENDIX B: CALCULATING THE ENERGY TRANSFER EFFICIENCY IN DNA

In fluorescence spectroscopy, absolute fluorescence quantum yield is normally defined as the ratio of the number of photons emitted to the number of the photons absorbed by the fluorophore. If we have a molecular system consisting of a fluorophore with one or more excitation energy donors, we must consider both direct excitation of the acceptor fluorophore and excitation of donor followed by transfer to acceptor. Let $A_a(\lambda_{ex})$, $A_d(\lambda_{ex})$, and $A(\lambda_{ex})$ be, respectively, the absorbance of the acceptor, the donors, and all absorbers (donors + acceptors). If we directly excite the acceptor (only) at wavelength λ_a (for 2AP, 305–330 nm would suffice), the fluorescence intensity measured would be $F_a(\lambda_a) = \Delta I_a(\lambda_a)\phi_0$, where $\Delta I_a(\lambda_a)$ is the number of photons per second absorbed by the acceptor and ϕ_0 is the normal fluorescence quantum yield, determined under the appropriate sample conditions (temperature, solvent, etc.). If we excite only donors (e.g., at 250–270 nm), which transfer to the acceptor with average efficiency $\eta_t(\lambda_d)$, the measured fluorescence intensity would be $F_d(\lambda_d) = \Delta I_d(\lambda_d)\eta_t(\lambda_d)\phi_0$. If we excite both donor and acceptor at some wavelength λ_{ex}, the fluorescence measured would be

$$F(\lambda_{ex}) = \left(\frac{A_a(\lambda_{ex})}{A(\lambda_{ex})} + \frac{A_d(\lambda_{ex})}{A(\lambda_{ex})}\,\eta_t(\lambda_{ex})\right)\Delta I(\lambda_{ex})\phi_0, \tag{B1}$$

where $\Delta I(\lambda_{ex})$ is the total number of photons absorbed per second. Note that $\Delta I_d = (A_d/A)\Delta I$ and $\Delta I_a = (A_a/A)\Delta I$. After some algebra, the average energy transfer efficiency from normal bases to 2AP in DNA oligomer can be written as

$$\eta_t(\lambda_{ex}) = \frac{A_a(\lambda_{ex})}{A_d(\lambda_{ex})}\left(\frac{F(\lambda_{ex})}{F_a(\lambda_{ex})} - 1\right), \tag{B2}$$

where $F(\lambda_{ex})$ is the fluorescence intensity of the oligomer, excited at wavelength λ_{ex}, $F_a(\lambda_{ex})$ is the fluorescence intensity of directly excited energy acceptor (2AP), $A_a(\lambda_{ex})$ is the absorbance of energy acceptor (2AP), and $A_d(\lambda_{ex})$ is the absorbance of energy donors (normal bases in DNA). $A_a(\lambda_{ex})$ and $F_a(\lambda_{ex})$ were measured from 2AP deoxynucleoside (dns); we multiplied the latter intensity by the ratio ϕ_0(2AP-dns)/ϕ_0(2AP in oligo) to

account for the yield difference between the two samples. Small differences between the spectra of directly excited 2AP in the oligo and 2AP-dns will cause errors in $\eta_t(\lambda_{ex})$ primarily above ~290 nm and below ~250 nm. A simpler approximation that does not require measurement of $F_a(\lambda_{ex})$, but which assumes no absorption spectral overlap between donor and acceptor, has been used earlier (Nordlund et al., 1993). Because we will always be determining ratios of fluorescence intensities of the same sample excited at different wavelengths, it is sufficient to simply measure the fluorescence signal from the fluorometer, which is proportional to the number of photons emitted per second.

APPENDIX C: CALCULATING THE TRANSFER EFFICIENCY FOR A PARTICULAR DNA BASE

Two types of transfer efficiencies in the DNA oligomer have been introduced: $\eta_t(\lambda)$ is the overall average transfer efficiency per donor from all donors (normal bases) to acceptor 2AP; $\eta_X(\lambda, n)$ is the transfer efficiency from a particular base type X (X = A, G, C, or T), located at position n, to 2AP. We number sites with the 2AP site located at $n = 0$, with negative integers indicating a site to the 5′ side of 2AP. From the average transfer efficiency, which comes more directly from experimental measurements, the transfer efficiency of a particular base to 2AP can be calculated through simple modeling. We make the assumption that the transfer efficiency to 2AP from a base adjacent to 2AP is not affected by the nature or number of other (normal) bases in the oligomer. This assumption may turn out to be incorrect when examined closely, but it allows a build-up of transfer rates starting from one reference oligomer. If this assumption were not allowed, the analysis would become unmanageable.

We start with the definition of average transfer efficiency (overall transfer efficiency per normal base) (Appendix A):

$$\eta_t(\lambda_{ex}) = \frac{\sum_X \sum_n^{Nx} \varepsilon_X(\lambda_{ex}, n)\eta_X(\lambda_{ex}, n)}{\sum_X \sum_n^{Nx} \varepsilon_X(\lambda_{ex}, n)} = \frac{\sum_X \sum_n^{Nx} \varepsilon_X(\lambda_{ex}, n)\eta_X(\lambda_{ex}, n)}{\varepsilon(\lambda_{ex})}. \quad (C1)$$

Nearest-neighbor transfer

To calculate the energy transfer efficiencies of particular bases, a 2AP-containing oligomer (CCC[2AP]CC) is used as a starting point. The base C is chosen because of the rather "generic" fluorescence spectra of oligomers with C adjacent to 2AP, indicating no strong interactions between C and 2AP on either side (Xu, 1996) and the relatively low transfer efficiency, again indicating relatively little specific interaction. Assuming that the absorption coefficient $\varepsilon(\lambda)$ of each base C is the same, then C1 can be written as

$$\eta_t(\lambda_{ex}) = \frac{\sum_{n=1}^5 \sum_{X=C} \varepsilon_X(\lambda_{ex}, n) \cdot \eta_X(\lambda_{ex}, n)}{\sum_{n=1}^5 \sum_{X=C} \varepsilon_X(\lambda_{ex}, n)} = \frac{1}{5}\sum_{n=1}^{5} \eta_C(\lambda_{ex}, n) = \frac{1}{5}(\eta_C(-3) + \eta_C(-2) + \eta_C(-1) + \eta_C(+1) + \eta_C(+2)), \quad (C2)$$

where $\eta_C(n)$ is the transfer efficiency of a particular base at position n in a single-stranded DNA and λ_{ex} has been dropped for clarity in the last expression. Here n is the nth position of the base X from energy acceptor 2AP. If only the nearest neighbors of 2AP significantly transfer, the average efficiency simplifies to

$$\eta_t(\lambda_{ex}) = \frac{1}{5}(\eta_C(-1) + \eta_C(+1)). \quad (C3)$$

If $\eta_C(-1) = \eta_C(+1)$, then $\eta_C(+1) = 11.8\%$ for $\eta_t(\lambda_{ex}) = 4.7\%$ (data at 5°C, $\lambda_{ex} = 260$ nm). Once the transfer efficiency of base C adjacent to 2AP on the right is calculated, the transfer efficiencies of other bases to the left of 2AP can be calculated as follows.

(1) CCX[2AP]CC, X = A, G, T oligomers

Similar to the derivation of Eqs. C2 and C3, the average transfer efficiency for these oligomers can be written as

$$\eta_t = \frac{\eta_C(-3) + \eta_C(-2) + \eta_C(+1) + \eta_C(+2) + g_X\eta_X(-1)}{4 + g_X} \cong \frac{\eta_C(+1) + g_X\eta_X(-1)}{4 + g_X}, \quad (C4)$$

where $g_X = \varepsilon_X/\varepsilon_C$ is a ratio of absorption coefficients, the wavelength dependence has been dropped for clarity, and the approximation is for nearest neighbors. At 5°C, values for g_X were $g_A = 2.08$, $g_G = 1.46$, $g_T = 1.16$. Because $\eta_t(\lambda)$ is available for all CCX[2AP]CC, X = A, G, T, from experiment and $\eta_C(+1) = 11.8\%$, the transfer efficiency of base X to the left of 2AP can be calculated as $\eta_A(-1) = 57.2\%$, $\eta_G(-1) = 19.2\%$, and $\eta_T(-1) = 10.3\%$.

(2) CCA[2AP]ACC oligomers

Because the transfer efficiency of base A at the left side of 2AP is now known, following the same procedure as before, the transfer efficiency of base A at the right side of 2AP can be calculated:

$$\eta_t = \frac{g_X[\eta_A(-1) + \eta_A(+1)]}{4 + 2g_X}, \quad (C5)$$

$$\eta_A(+1) = \frac{(4 + 2g_A)}{g_A}\eta_t + \eta_A(-1). \quad (C6)$$

For $\eta_t = 29.3\%$ and $\eta_A(-1) = 57.2\%$, $\eta_A(+1) = 57.7\%$. The approximate equality of $\eta_A(-1)$ and $\eta_A(+1)$ supports the earlier assumption, $\eta_C(-1) = \eta_C(+1)$.

Next-nearest neighbor transfer. Now we make the zeroth-order calculation for transfer from bases twice removed from 2AP. (We will not attempt here to go back and calculate the correction on the nearest-neighbor efficiency from the presence of this term, although that can clearly be done. The correction will be small (within our error bars) if the second-nearest-neighbor transfer efficiency is much smaller than the nearest-neighbor transfer efficiency.)

(3) CCAX[2AP]CC, X = A, G, C, and T oligomers

From Eq. C1, the average transfer efficiency can be written as

$$\eta_t = \frac{\varepsilon_A\eta_A(-2) + \varepsilon_X\eta_X(-1) + \varepsilon_C\eta_C(+1)}{4\varepsilon_C + \varepsilon_X + \varepsilon_A}. \quad (C7)$$

In the above equation all terms but $\eta_A(-2)$ are now known; therefore, $\eta_A(-2)$ can be calculated. For any other particular base twice removed

from 2AP in the single-stranded oligomer, the transfer efficiency can be calculated by the same procedure as above. The approach to calculating transfer from bases even farther removed is evident.

APPENDIX D: TRANSFER IN DOUBLE-STRANDED DNA

The overall transfer efficiency per donor for the double-stranded DNA decamer d(AAAA[2AP]AAAAA/TTTTTTTTTT) is

$$\eta_{ds} = \frac{\varepsilon_{A,ds}\eta^{sum}_{A,ds}}{9\varepsilon_{A,ds} + 10\varepsilon_{T,ds}}, \quad \text{(D1)}$$

where transfer from T in the second (n') strand to 2AP in the first (n) strand has been neglected, as supported by measurements, and the superscript "sum" refers to the sum of all A-to-2AP efficiencies. (Recall that we are looking for the effect on transfer within the first strand of addition of the complementary strand.) The ratio of the two overall energy transfer efficiencies is

$$r = \frac{\eta_{ds}}{\eta_{ss}} = \frac{9\varepsilon_A}{10\varepsilon_T + 9\varepsilon_A}\frac{\eta^{sum}_{A,ds}}{\eta^{sum}_{A,ss}}. \quad \text{(D2)}$$

Using absorption coefficients from Borer (1975), the ratio r is

$$r = 0.60\,\frac{\eta^{sum}_{A,ds}}{\eta^{sum}_{A,ss}} \quad \text{(D3)}$$

for this decamer. So there are three cases: 1) if $r > 0.60$, forming the double helix (base pairing) facilitates the energy transfer in the 2AP-containing strand ($\eta^{ds}_{sum} > \eta^{ss}_{sum}$); 2) if $r \approx 0.60$, base pairing does not affect the energy transfer in the 2AP-containing strand ($\eta^{ds}_{sum} = \eta^{ss}_{sum}$); 3) if $r < 0.60$, base pairing reduces the energy transfer in the 2AP-containing strand ($\eta^{ds}_{sum} < \eta^{ss}_{sum}$).

Supported in part by National Science Foundation grant MCB-9723278 and National Institutes of Health grant AR41877-01.

REFERENCES

Allan, B. W., N. O. Reich, and J. M. Beechem. 1999. Measurement of the absolute temporal coupling between DNA binding and base flipping. *Biochemistry.* 38:5308–5314.

Ballini, J.-P., M. Daniels, and P. Vigny. 1982. Wavelength-resolved lifetime measurements of emission from DNA components and poly rA at room temperature excited with synchrotron radiation. *J. Lumin.* 27: 389–400.

Ballini, J.-P., M. Daniels, and P. Vigny. 1988. Synchrotron-excited time-resolved fluorescence spectroscopy of adenosine, protonated adenosine and 6N,6N-dimethyladenosine in aqueous solution at room temperature. *Eur. Biophys. J.* 16:131–142.

Ballini, J.-P., P. Vigny, G. Thomas, and A. Favre. 1976. Intramolecular energy transfer in native tRNA at room temperature. *Photochem. Photobiol.* 24:321–329.

Bergmanson, J. P., and T. M. Sheldon. 1997. Ultraviolet radiation revisited. *CLAO J.* 23:196–204.

Bloomfield, V., D. Crothers, and J. I. Tinoco. 1974. Physical Chemistry of Nucleic Acids. Harper and Row, New York.

Borer, P. N. 1975. Optical properties of nucleic acids: absorption and circular dichroism spectra. *In* Handbook of Biochemistry and Molecular Biology. G. D. Fasman, editor. CRC Press, Cleveland. 589–590.

Brash, D. E., and W. A. Haseltine. 1982. UV-induced mutation hotspots occur at DNA damage hotspots. *Nature.* 298:189–192.

Brunk, C. F. 1973. Distribution of dimers in ultraviolet-irradiated DNA. *Nature New Biol.* 241:74–76.

Burr, J. G., W. A. Summers, and Y. S. Lee. 1975. Energy transfer in fluorescent derivatives of uracil and thymine. *J. Am. Chem. Soc.* 97: 245–248.

Callis, P. R. 1979. Polarized fluorescence and estimated lifetimes of the DNA bases at room temperature. *Chem. Phys. Lett.* 61:563–567.

Callis, P. R. 1983. Electronic states and luminescence of nucleic acid systems. *Annu. Rev. Phys. Chem.* 34:329–357.

Daniels, M., and W. Hauswirth. 1971. Fluorescence of the purine and pyrimidine bases of the nucleic acids in neutral aqueous solution at 300 degrees K. *Science.* 171:675–677.

Evans, K., D.-G. Xu, Y.-S. Kim, and T. M. Nordlund. 1992. 2-Aminopurine optical spectra: solvent, pentose ring and DNA helix melting dependence. *J. Fluorescence.* 2:209–216.

Evans, K. O. 1998. Dynamic characterization of 2-aminopurine in oligonucleotides using fluorescence, magnetic resonance, and Raman spectroscopies. Ph.D. thesis. University of Alabama at Birmingham, Birmingham, AL.

Fisher, G. J., Z. Q. Wang, S. C. Datta, J. Varani, S. Kang, and J. J. Voorhees. 1997. Pathophysiology of premature skin aging induced by ultraviolet light. *N. Engl. J. Med.* 337:1419–1428.

Frank-Kamenetskii, M. D., and Y. S. Lazurkin. 1974. Conformational changes in DNA molecules. *Annu. Rev. Biophys. Bioeng.* 3:127–150.

Ge, G., and S. Georghiou. 1991a. Excited-state properties of the alternating polynucleotide poly(dA-dT) · poly(dA-dT). *Photochem. Photobiol.* 54: 301–305.

Ge, G., and S. Georghiou. 1991b. Room-temperature fluorescence properties of the polynucleotide polydA · polydT. *Photochem. Photobiol.* 54:477–480.

Georghiou, S., T. M. Nordlund, and A. M. Saim. 1985. Picosecond fluorescence decay time measurements of nucleic acids at room temperature in aqueous solution. *Photochem. Photobiol.* 41:209–212.

Georghiou, S., S. Zhu, R. Weidner, C.-R. Huang, and G. G. 1990. Singlet-singlet energy transfer along the helix of a double-stranded nucleic acid at room temperature. *J. Biomol. Struct. Dyn.* 8:657–674.

Gordon, L. K., and W. A. Haseltine. 1982. Quantitation of cyclobutane pyrimidine dimer formation in double- and single-stranded DNA fragments of defined sequence. *Radiat. Res.* 89:99–112.

Gräslund, A., F. Claesens, L. W. McLaughlin, P.-O. Lycksell, U. Larsson, and R. Rigler. 1987. NMR and time-resolved fluorescence studies of a 2-aminopurine substituted *Eco*RI restriction site. *In* Structure, Dynamics and Function of Biomolecules. A. Ehrenberg, R. Rigler, A. Gräslund, and L. Nilsson, editors. Springer-Verlag, Berlin. 201–207.

Gueron, M., J. Eisinger, and A. A. Lamola. 1974. Excited states of nucleic acids. *In* Basic Principles in Nucleic Acid Chemistry. P. O. P. T'so, editor. Academic Press, New York. 311–398.

Gueron, M., J. Eisinger, and R. G. Schulman. 1967. Excited states of nucleotides and singlet energy transfer in polynucleotides. *J. Chem. Phys.* 47:4077–4091.

Hauswirth, W. W., and M. Daniels. 1976. Excited states of the nucleic acids: polymeric forms. *In* Photochemistry and Photobiology of Nucleic Acids. S.-Y. Wang, editor. Academic Press, New York. 109–167.

Hauswirth, W., and S.-Y. Wang. 1977. Excited state processes and solution conformation of dipyrimidine adducts. *Photochem. Photobiol.* 25: 161–166.

Holz, B., S. Klimasauskas, S. Serva, and E. Weinhold. 1998. 2-Aminopurine as a fluorescent probe for DNA base flipping by methyltransferases. *Nucleic Acids Res.* 26:1076–1083.

Huang, C.-R., and S. Georghiou. 1992. Room-temperature steady-state fluorescence properties of poly(dG-dC) · poly(dG-dC). *Photochem. Photobiol.* 56:95–99.

Kakitani, T., A. Kimura, and H. Sumi. 1999. Theory of excitation transfer in the intermediate coupling case. *J. Phys. Chem. B.* 103:3720–3726.

Kelley, S. O., and J. K. Barton. 1999. Electron transfer between bases in double helical DNA. *Science.* 283:375–381.

Kobayashi, S., M. Yamashita, T. Sato, and S. Muramatsu. 1984. Single-photon sensitive synchroscan streak camera for room temperature pico-

second emission dynamics of adenine and polyadenylic acid. *IEEE J. Quantum Electron.* QE-20:1383–1386.

Lamola, A. A. 1969. Specific formation of thymine dimers in DNA. *Photochem. Photobiol.* 9:291–294.

Le Pecq, J. B., and C. Paoletti. 1967. A fluorescent complex between ethidium bromide and nucleic acids. Physical-chemical characterization. *J. Mol. Biol.* 27:87–106.

Lerman, L. S. 1963. The structure of the DNA-acridine complex. *Proc. Natl. Acad. Sci. USA.* 49:94–102.

Lycksell, P. O., A. Gräslund, F. Claesens, L. W. McLaughlin, U. Larsson, and R. Rigler. 1987. Base pair opening dynamics of a 2-aminopurine substituted *Eco*RI restriction sequence and its unsubstituted counterpart in oligonucleotides. *Nucleic Acids Res.* 15:9011–9025.

McLaughlin, L. W., T. Leong, F. Benseler, and N. Piel. 1988. A new approach to the synthesis of a protected 2-aminopurine derivative and its incorporation into oligodeoxynucleotides containing the *Eco*RI and *Bam*HI recognition sites. *Nucleic Acids Res.* 16:5631–5644.

Millar, D. P., and L. C. Sowers. 1990. Sequence-dependent dynamics of DNA. *Proc. SPIE.* 1204:656–662.

Mitchell, D. L. 1988. The relative cytotoxicity of (6-4) photoproducts and cyclobutane dimers in mammalian cells. *Photochem. Photobiol.* 48: 51–57.

Nordlund, T. M. 1988. Streak camera methods in nucleic acid and protein fluorescence spectroscopy. *Proc. SPIE.* 909:35–50.

Nordlund, T. M. 1990. Time-resolved fluorescence of nucleic acids. *In* Nonlinear Optics and Ultrafast Phenomena. R. R. Alfano and L. Rothberg, editors. Nova Publishing, New York. 83–88.

Nordlund, T. M. 1991. Streak cameras for time-domain fluorescence. *In* Fluorescence Spectroscopy: Principles and Applications, Vol. 1, Principles and Techniques. J. R. Lakowicz, editor. Plenum Press, New York. 183–260.

Nordlund, T. M., S. Andersson, L. Nilsson, R. Rigler, A. Gräslund, and L. W. McLaughlin. 1989. Structure and dynamics of a fluorescent DNA oligomer containing the *Eco*RI recognition sequence: fluorescence, molecular dynamics and NMR studies. *Biochemistry.* 28:9095–9103.

Nordlund, T. M., P. Wu, S. Andersson, L. Nilsson, R. Rigler, A. Gräslund, L. W. McLaughlin, and B. Gildea. 1990. Structural dynamics of DNA sensed by fluorescence from chemically-modified bases. *Proc. SPIE.* 1204:344–353.

Nordlund, T. M., D. Xu, and K. Evans. 1994. Conformation, motion and base-to-base excitation energy transfer in DNA. *Proc. SPIE.* 2137: 634–643.

Nordlund, T. M., D. Xu, and K. O. Evans. 1993. Excitation energy transfer in DNA: duplex melting and transfer from normal bases to 2-aminopurine. *Biochemistry.* 32:12090–12095.

Oraevsky, A. A., A. V. Sharkov, and D. N. Nikogosyan. 1981. Picosecond study of electronically excited singlet states of nucleic acid components. *Chem. Phys. Lett.* 83:276–280.

Patrick, M. H., and R. O. Rahn. 1976. Photochemistry of DNA and polynucleotides: photoproducts. *In* Photochemistry and Photobiology of Nucleic Acids. S.-Y. Wang, editor. Academic Press, New York. 35–95.

Randle, H. W. 1997. Suntanning: differences in perceptions throughout history. *Mayo Clin. Proc.* 72:461–466.

Rigler, R., and F. Claesens. 1986. Picosecond time domain spectroscopy of structure and dynamics in nucleic acids. *In* Structure and Dynamics of DNA. P. H. van Knippenberg and C. W. Hillers, editors. Plenum Press, New York. 45–54.

Rigler, R., F. Claesens, and O. Kristensen. 1985. Picosecond fluorescence spectroscopy in the analysis of structure and motion of biopolymers. *Anal. Instrum.* 14:525–546.

Rubin, Y. V., and S. A. Yegupov. 1987. Effect of intramolecular interaction on the electron excitation state of nucleic acid components. *Biophysics (Poland).* 32:409–413.

Setlow, J. K., and R. B. Setlow. 1961. Ultraviolet action spectra of ordered and disordered DNA. *Proc. Natl. Acad. Sci. USA.* 47:1619–1627.

Shafranovskaya, N. N., E. N. Trifonov, Y. S. Lazurkin, and M. D. Frank-Kamenetskii. 1973. *Nature New Biol.* 241:58–60.

Suhai, S. 1984. First principles charge transfer exciton theory of the UV spectrum of DNA. *Int. J. Quantum Chem. Quantum Biol. Symp.* 11: 223–235.

Sutherland, B. M., and J. C. Sutherland. 1967. Mechanisms of inhibition of pyrimidine dimer formation in deoxyribonucleic acid by acridine dyes. *Biophys. J.* 9:292–302.

Umlas, M. E., W. A. Franklin, G. L. Chan, and W. A. Haseltine. 1985. Ultraviolet light irradiation of defined-sequence DNA under conditions of chemical photosensitization. *Photochem. Photobiol.* 42:265–273.

Urbach, F. 1997. Ultraviolet radiation and skin cancer of humans. *J. Photochem. Photobiol. B Biol.* 40:3–7.

Varghese, A. J. 1972. Photochemistry of nucleic acids and their constituents. *Photophysiology.* 7:207–274.

Varghese, A. J., and S. Y. Wang. 1967. Ultraviolet irradiation of DNA in vitro and in vivo produces a 3d thymine-derived product. *Science.* 156:955–957.

Vigny, P., and J. P. Ballini. 1977. Excited states of nucleic acids at 300K and electronic energy transfer. *In* Excited States in Organic Chemistry and Biochemistry. B. Pullman and N. Goldblum, editors. D. Reidel Publishing Co., Dordrecht, The Netherlands. 1–13.

Voet, D., W. B. Gratzer, R. A. Cox, and P. Doty. 1963. Absorption spectra of nucleotides, polynucleotides, and nucleic acids in the far ultraviolet. *Biopolymers.* 1:193–208.

Wang, S.-Y. 1976. Pyrimidine bimolecular photoproducts. *In* Photochemistry and Photobiology of Nucleic Acids. S.-Y. Wang, editor. Academic Press, New York. 295–356.

Wang, S.-Y. 1980. Separation of cyclobutyl dimers of thymine and thymidine by high-performance liquid chromatography and thin-layer chromatography. *J. Chromatogr.* 195:139–145.

Ward, D. C., E. Reich, and L. Stryer. 1969. Fluorescence studies of nucleotides and polynucleotides. *J. Biol. Chem.* 244:1228–1237.

Weill, G., and M. Calvin. 1963. Optical properties of chromophore-macromolecule complexes: absorption and fluorescence of acridine dyes bound to polyphosphates and DNA. *Biopolymers.* 1:401–417.

Xu, D. 1996. Sequence dependent energy transfer in DNA oligonucleotides. Ph.D. thesis. University of Alabama at Birmingham, Birmingham, AL.

Xu, D., K. O. Evans, and T. M. Nordlund. 1994. Melting and premelting transitions of oligomers measured by DNA base fluorescence and absorption. *Biochemistry.* 33:9592–9599.